Interaction Notes

Note 325

Electromagnetic Pulse Penetration Through Dielectric Skin Panels on the Leading Edge of Aircraft Wings

May 1977

A.D. Varvatsis and M.I. Sancer

TDR, Inc.
Los Angeles, California

Abstract

EMP penetration through the dielectric skin panels covering part of the leading edge of the wings on an aircraft is considered in this report. Approximate expressions and simplified estimates are derived for the current and voltage induced on conductors housed in the wing cavity. These expressions are functions of the geometry and the longitudinal current and charge densities evaluated at the short-circuited apertures. These densities must be supplied by a separate external interaction analysis.

ACKNOWLEDGMENT

We thank Scott Siegel for his contribution to appendix B and Kelvin Lee for helpful discussions.

SECTION I

INTRODUCTION

Penetration of electromagnetic pulse energy through the various ports of entry on an aircraft and the assessment of its effects on mission critical subsystems is a subject of importance. In this report, energy leakage through the dielectric skin panels covering part of the leading edge of the wings of an aircraft is considered and approximate expressions and simplified estimates are derived for the currents and voltages induced on conductors housed in the leading edge of the wing cavity. These panels are made of fiberglass and are supported by metal ribs as shown in figure 1. The task is to calculate the current and voltage induced on the pneumatic duct and also the current induced on the unshielded cables spaced uniformly and set against the partition wall which, along with the leading edge, form a wing cavity cross section of approximately triangular shape. The task is accomplished as follows: In section II the formulation and solution is presented for low frequency penetration through a periodic array of apertures into a cylindrical waveguide that can support a TEM mode and this is related to the manner in which the wing cavity is approximated. As a model for the aircraft the one developed in reference 1 can be used but any other model or experimental results can be used since the formulas involve the longitudinal current density and charge density induced on the short-circuited apertures due to the EMP interaction with the aircraft. Knowledge of the external interaction

---

1. Sancer, M. I., S. Siegel and A. D. Varvatsis, Foundation of the Magnetic Field Integral Equation Code for the Calculation of Electromagnetic Pulse External Interaction with Aircraft, (to be published as Interaction Note 320) Air Force Weapons Laboratory, December 1976.

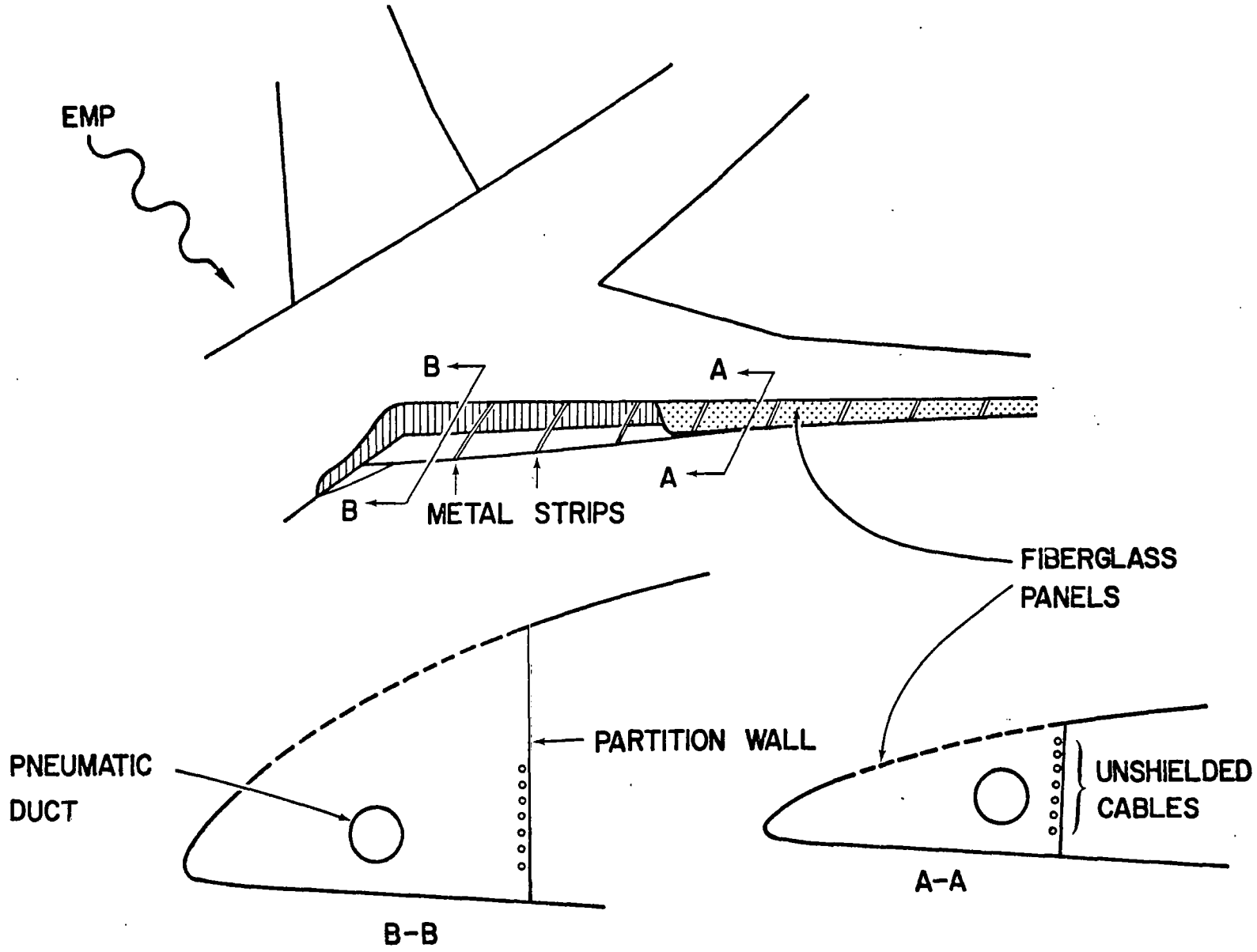

Figure 1. Various Configurations Constituting the Geometry of the EMP Penetration Problem

quantities is necessary for the calculation of the equivalent voltage and current forcing functions at the site of the apertures. The method employed to calculate the induced TEM currrent and voltage follows a formulation found in reference 2 and is developed in a manner similar to the one used in reference 3. In section III the TEM parameters are calculated for a cylinder with a triangular cross section housing an inner circular conductor and also the current induced on the cables near the partition wall. In section IV the results are displayed in a compact form that allows the induced currents and voltages to be calculated without any reference to the rest of this report except appendix B in which calculations are given of the aperture polarizabilities. In the same section the E-4 aircraft is considered, whose pertinent dimensions are known, and simplified formulas for the induced current and voltage are given. Finally, appendix A provides a derivation for the magnetic and electric dipole moments in terms of the aperture electric field for the problem of low frequency penetration through an aperture in a perfectly conducting planar screen and appendix B calculates the magnetic and electric polarizabilities for a periodic array of rectangular apertures in a perfectly conducting planar screen.

---

2. Van Bladel, J., Electromagnetic Fields, McGraw-Hill Book Company, New York, p. 418, 1964.

3. Lee, K.S.H. and C. E. Baum, "Application of Modal Analysis to Braidel-Shield Cables," Interaction Note 132, Air Force Weapons Laboratory, January 1973.

SECTION II

FORMULATION AND SOLUTION

The configuration we are considering in this report is depicted in figure 1. We assume that an EMP of arbitrary direction and polarization is incident on the airplane and we wish to calculate the currents induced on the pneumatic duct and wiring cables due to the EMP penetration through the fiberglass skin. Naturally, the complexity of the structure makes this calculation a formidable if not impossible task. To be able to obtain a useful estimate of the induced currents without excessive labor we have to make model idealizations and also seek approximate solutions. Some of these idealizations and approximations will be given shortly. The rest will be presented as we formulate and solve the problem later on in this section.

1. For the external interaction problem we need to know the short-circuited current and charge densities at the location of the apertures. These quantities can be obtained either experimentally or analytically by modeling the aircraft in a certain manner. For example, the wings, fuselage, horizontal and vertical stabilizers can be modeled as perfectly conducting elliptical cylinders. Such a model of an aircraft has been employed in reference 1 to study the external interaction of EMP with aircraft and consequently we can utilize the results of this study to calculate the total tangential magnetic field (or equivalently current density) and perpendicular electric field (or equivalently charge density) on the surface of the wing. These quantities, as we will explain later, can serve as inputs for the calculation of the current

induced on the interior conductors due to penetration of the EMP through the apertures on the wing.

2. We will neglect the effect of the fiberglass skin covering the apertures and assume air instead. Thus the penetration takes place through the apertures separated by the metallic dividers or ribs shown in figure 1. By setting the dielectric constant of the fiberglass skins equal to one we actually overestimate the amount of energy leaking into the wing cavity and consequently this calculation provides an upper bound.

3. For the interior problem, the wing cavity will be approximated by a perfectly conducting cylinder with a triangular cross section. The pneumatic duct and the triangular cavity cross section form the cross section of a doubly connected region which can support a TEM mode. It is this mode only that we will consider in our subsequent calculations. Notice that for the calculation of the TEM mode we will ignore the presence of any other conductors. In particular, the wiring cables are replaced by the partition wall shown in figure 1. The current induced on the cables will be estimated, as we will explain later in detail, by calculating $\hat{n} \times \underline{H}$ on the partition wall times the diameter of the cable. The justification for ignoring the TM and TE modes that can be excited relies on the fact that for the bulk of the EMP energy the frequencies involved are sufficiently low to only excite evanescent TM and TE modes; consequently their energy cannot significantly propagate down the waveguide (and into circuitry) a few radii away from the apertures. (By radius we mean the average linear dimension of the wing cavity cross section. See section IV for more details.)

We will now outline the formulation and solution to our problem. We will start with an exact set of equations involving the TEM magnetic and electric field coefficients (within a cylindrical waveguide that can support a TEM mode) and the axial component of the total electric field evaluated at the apertures on the surface of the guide. Next we will relate the usual voltage V(z) and current I(z) definitions to the TEM coefficients and thus obtain a set of exact equations relating V(z), I(z) to the z-component of the total electric field at the apertures. Theoretically, this component of the electric field can be obtained in two steps. First we solve the exterior problem, i.e., the interaction of the EMP with the cylinder (or the aircraft in our case) provided we short circuit all apertures on the surface of the body. This calculation gives the current density distribution $\underline{J}_{s.c.}$ on the body and in particular on the location of the short-circuited apertures. The second step requires knowledge of the exterior and interior Green's function that allow the derivation of an integral equation for the total aperture electric field in terms of the current density distribution on the location of the short-circuited apertures calculated in step one. (Solving this equation numerically also requires knowledge of the short-circuited charge density.) Reference 1 has derived a computer code calculating $\underline{J}_{s.c.}$ for the aircraft model described earlier in this section. For our purposes the axial aperture field E_z will not be directly calculated. For wavelengths large compared to the dimensions of an aperture, A, one need only calculate

$$\int_A E_z^{(1)}\, dS \quad \text{and} \quad \int_A E_z^{(0)}\, z dS$$

where $E_z^{(1)}$ and $E_z^{(0)}$ are the first order and zeroth order aperture electric field respectively. These integrals are

proportional to the magnetic dipole moment and electric dipole moment respectively. The details of their calculation and concomitant approximations will be given later on in this section. These moments act as sources for the excitation of the TEM mode, the detailed calculation of which will now be given.

We start with equations (13.8) in reference 2, for an $e^{-i\omega t}$ time dependence, valid in a cylindrical waveguide that can support a TEM mode (fig. 2) and for now assume that there is one aperture only.

$$\frac{da_o}{dz} - i\omega\mu_o\alpha_o = \frac{1}{N_o^2}\int_c E_z \frac{\partial\phi_o}{\partial n}\, dc$$

$$\frac{d\alpha_o}{dz} - i\omega\epsilon_o a_o = 0 \qquad (1)$$

where E_z is the z-component of the total aperture electric field and a_o, α_o are expansion coefficients for the TEM mode electric and magnetic fields respectively such that

$$\underline{e}_{TEM} = a_o(z)\ \nabla_t\phi_o$$

$$\underline{h}_{TEM} = \alpha_o(z)\ \hat{e}_z \times \nabla_t\phi_o \qquad (2)$$

where ∇_t is the two-dimensional gradient operator $(\partial/\partial x)\hat{e}_x + (\partial/\partial y)\hat{e}_y$. The integration in Equation 1 is over a contour c as indicated in figure 2, i.e., a contour passing through the aperture A at location z = z. The normalization constant N_o^2 is given by

$$N_o^2 = \int_S |\nabla_t\phi_o|^2\, dS \qquad (3)$$

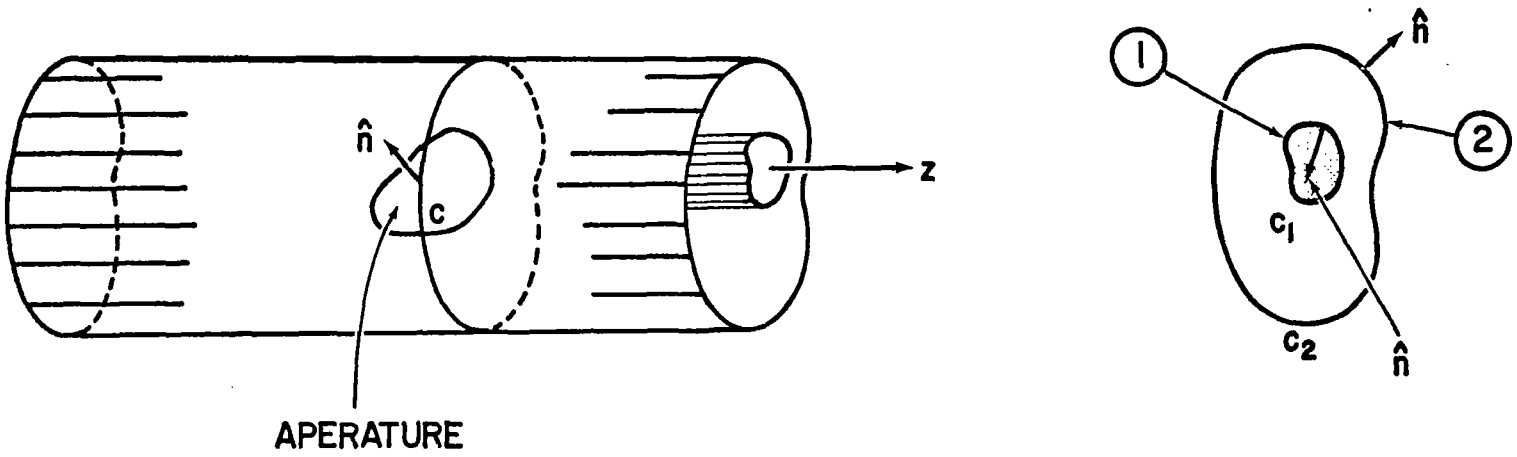

Figure 2. Geometry for TEM Excitation Through an Aperture

and ϕ_o satisfies Laplace's equation over the waveguide cross section:

$$\nabla_t^2 \phi_o(x,y) = 0 \qquad x,y \in S \tag{4}$$

with boundary conditions

$$\phi_o(2) = 0 \qquad \phi_o(1) = 1. \tag{5}$$

To relate a_o and α_o to the usual definitions for voltage and current we recall that

$$V(z) = \int_2^1 \underline{e}_{TEM} \cdot \underline{d\ell} = \int_2^1 a_o(z)\ \nabla_t \phi_o \cdot \underline{d\ell}$$

$$= a_o(z)\ [\phi_o(1) - \phi_o(2)] = a_o(z) \tag{6}$$

and from figure 2

$$I(z) = \oint_{C_1} \underline{h}_{TEM} \cdot \underline{d\ell} = \oint_{C_1} \alpha_o(z)\ \hat{e}_z \times \nabla_t \phi_o \cdot \underline{d\ell}$$

$$= \alpha_o(z) \oint_{C_1} \frac{\partial \phi_o}{\partial n}\, d\ell\ . \tag{7}$$

We will now show that N_o^2 given by Equation 3 is equal to the integral in Equation 7. We start with the identity

$$\nabla_t \cdot (\phi_o \nabla_t \phi_o) = |\nabla_t \phi_o|^2 + \phi_o \nabla_t^2 \phi_o$$

$$= |\nabla_t \phi_o|^2\ .$$

Integrating both sides over the cross section S and using Gauss' theorem we obtain

$$\int_S \nabla_t \cdot (\phi_o \nabla_t \phi_o)\, dS = \oint_{c_1+c_2} \phi_o \frac{\partial \phi_o}{\partial n}\, d\ell = \int_S |\nabla_t \phi_o|^2\, dS \qquad (8)$$

where $\hat{n}$ is the outward normal (fig. 2). Recalling that $\phi_o(2) = 0$, $\phi_o(1) = 1$, we finally arrive at the desired relationship

$$\oint_{c_1} \frac{\partial \phi_o}{\partial n}\, d\ell = \int |\nabla_t \phi_o|^2\, dS = N_o^2 \qquad (9)$$

and

$$I(z) = \alpha_o(z)\, N_o^2 \,. \qquad (10)$$

In view of Equations 8 and 10, Equation 1 becomes

$$\frac{dV}{dz} - i\omega L I = \frac{L}{\mu_o} \int_c E_z \frac{\partial \phi_o}{\partial n}\, dc$$

$$\frac{dI}{dz} - i\omega C V = 0 \qquad (11)$$

where

$$L = \frac{\mu_o}{N_o^2} \qquad C = \varepsilon_o N_o^2 \qquad (12)$$

are the inductance and capacitance per unit length for the transmission line corresponding to the TEM mode of the waveguide structure. These quantities are explicitly calculated

in the next section. The above set of Equations 11 has also been derived in reference 3 via a somewhat different approach.

From Equations 11 one easily obtains

$$\frac{d^2I}{dz^2} + k^2 I = i\omega\epsilon_o \int_c E_z \frac{\partial\phi_o}{\partial n}\, dc \qquad (13)$$

where $k^2 = \omega^2\mu_o\epsilon_o$.

The particular solution of Equation 13 can be found with the aid of the one-dimensional Green's function $G(z,z') = (1/2ik)\exp[ik|z-z'|]$ representing outgoing waves at $z = \pm\infty$

$$I = \frac{1}{2ik}\int_{-\infty}^{\infty} f(z')\, e^{ik|z-z'|}\, dz'$$

$$= \frac{1}{2Z_o}\int_A E_z(z')\, \frac{\partial\phi_o}{\partial n}\, e^{ik|z-z'|}\, dS' \qquad (14)$$

where $f(z)$ is the source term in Equation 13, $Z_o = (\mu_o/\epsilon_o)^{1/2}$ and A is the aperture. Assuming that $(\partial\phi_o/\partial n)$ does not vary appreciably over the aperture (the contour c) Equation 14 can be rewritten as

$$I(z) = \frac{1}{2Z_o}\frac{\partial\phi_o}{\partial n}\int_A E_z(z')\, e^{ik|z-z'|}\, dS'. \qquad (15)$$

We will simplify Equation 15 by considering two cases: $z > b$ and $z < -b$ (fig. 3). For $z > b$ Equation 15 gives

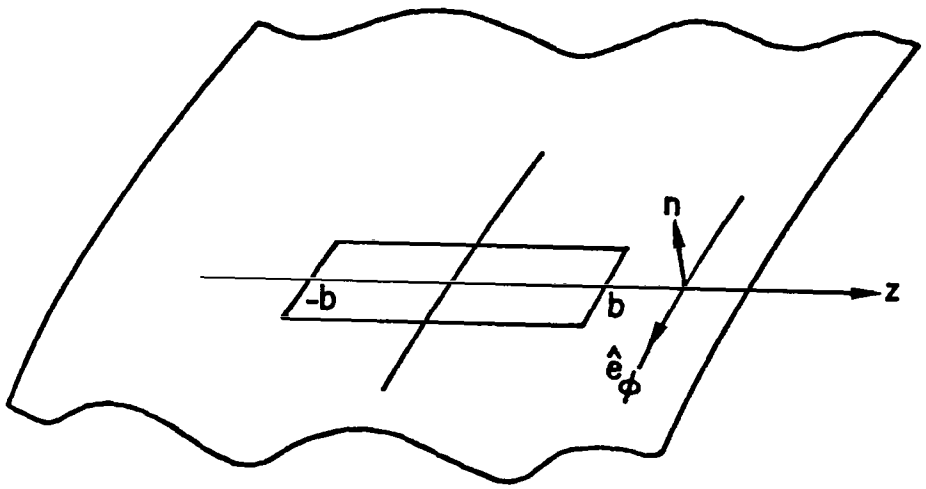

Figure 3. A Rectangular Aperture on the Outer Conductor of a Cylindrical Waveguide

$$I(z) = \frac{1}{2Z_o} \frac{\partial \phi_o}{\partial n} e^{ikz} \int_A E_z(z')\, e^{-ikz'}\, ds' \qquad (16)$$

Assuming now that $2kb << 1$, i.e., that the linear dimension of the aperture $2b$ is much smaller than $\lambda/2\pi$ where λ is the wavelength, we can expand $\exp(-ikz')$ and only keep two terms

$$I(z) = \frac{1}{2Z_o} \frac{\partial \phi_o}{\partial n} e^{ikz} \left\{ \int_A E_z(z')\, ds' - ik \int_A E_z(z')\, z'\, ds' \right\} . \qquad (17)$$

To relate these integrals to the magnetic and electric moments, as we suggested earlier, we make some pertinent calculations. First we show that

$$\int_A \hat{n} \times \underline{E}\, dS = i\omega\mu_o \int_A \underline{r}_s\, \hat{n} \cdot \underline{H} dS \qquad (18)$$

where $\hat{n}$ is the unit normal to the aperture surface and $\underline{r}_s$ the radius vector at points on the surface. (The exact shape of the surface is not important, but it usually matches the rest of the metallic surface.) To arrive at Equation 18 we use

$$\nabla_t \cdot (\hat{n} \times \underline{E}\, \underline{r}_s) \equiv \underline{r}_s \nabla_t \cdot (\hat{n} \times \underline{E}) + \hat{n} \times \underline{E}$$

$$\underline{E} \cdot \hat{u} = 0$$

(where $\hat{u}$ is the tangential unit vector at the edge of the aperture) and Gauss' theorem on a surface to obtain

$$\int_A \hat{n} \times \underline{E}\, dS = - \int_A \underline{r}_s \nabla_t \cdot (\hat{n} \times \underline{E})\, dS. \qquad (19)$$

Next we recall that $\nabla \times \underline{E} = i\omega\mu_o \underline{H}$ and use the identity $\nabla_t \cdot (\hat{n} \times \underline{E}) \equiv -\hat{n} \cdot \nabla_t \times \underline{E}_t + \underline{E} \cdot \nabla_t \times \hat{n}$ to obtain

$$\nabla_t \cdot (\hat{n} \times \underline{E}) = -i\omega\mu_o \hat{n} \cdot \underline{H} . \tag{20}$$

(One can show that $\nabla_t \times \hat{n} = 0$ on a surface.) Combining Equations 19 and 20 we arrive at Equation 18. If $\hat{e}_\phi$ is a unit vector on the surface of the wing along a direction perpendicular to z we can write

$$\hat{n} \times \underline{E} = - \hat{e}_\phi E_z + E_\phi \hat{e}_z \tag{21}$$

and

$$\int_A E_z dS = \left[-i\omega\mu_o \int_A \underline{r}_s \hat{n} \cdot \underline{H} \, dS \right] \cdot \hat{e}_\phi . \tag{22}$$

If we expand E_z and $\underline{H}$ in a power series in ik we have

$$E_z = E_z^{(0)} + E^{(1)} + \ldots$$

$$\underline{H} = \underline{H}^{(0)} + \underline{H}^{(0)} + \tag{23}$$

where the nth term is proportional to $(ik)^n$ and from Equation 22 we see that

$$\int_A E_z^{(0)} \, dS = 0$$

$$\int_A E_z^{(1)} \, dS = \left[-i\omega\mu_o \int_A \underline{r}_s \hat{n} \cdot \underline{H}^{(0)} \, dS \right] \cdot \hat{e}_\phi . \tag{24}$$

If we recall that we only kept the first two terms in the expansion for exp (-ikz') we understand that in the calculation of $\int_A E_z \, dS$ we must use no higher order terms than first and in the calculation of $\int z' \, E_z \, dS$, E_z must be the electrostatic field. From Equations 22 and 24 we see that we need only know $\underline{H}$ to zeroth order for the calculation of $\int E_z \, dS$. Thus we can evaluate the integrals in Equation 17 by solving an electrostatic and magnetostatic problem.

One defines

$$\underline{m} \equiv -\frac{1}{i\omega\mu_o} \int_A \hat{n} \times \underline{E} \, dS = -\int_A \underline{r}_s \, \hat{n} \cdot \underline{H} \, dS \tag{25}$$

as the imaged magnetic moment and consequently

$$\int_A E_z \, dS = i\omega\mu_o \, \underline{m} \cdot \hat{e}_\phi. \tag{26}$$

We will now relate the second integral $\int_A E_z \, z' dS$ to the imaged electric dipole moment $\underline{p}$.

One defines

$$\underline{p} \equiv -\frac{\varepsilon_o}{2} \int_A \underline{r}_s \cdot \underline{E} \, \hat{n} dS. \tag{27}$$

Definitions 25 and 27 owe their origin to the problem of low-frequency penetration through an aperture in a perfectly conducting planar screen. If one places both $\underline{m}$ and $\underline{p}$ in front of the short circuited planar aperture, the far zone fields in the transmission side due to the dipoles are equal to the far zone transmitted fields for the original penetration problem. (See Appendix A.) As we found earlier, we need only calculate E_z in $\int_A E_z \, z' dS$ to zeroth order. Thus we can

set $\underline{E} = -\nabla\psi$ where ψ satisfies Laplace's equation with $\psi = 0$ on the conducting screen.

If we expand $\underline{r}_s \cdot \underline{E}$

$$\underline{r}_s \cdot \underline{E} = zE_z + pE_p$$

where p is a coordinate orthogonal to z ($E_p \equiv E_\phi$) we can show that

$$\int_A z'E_z \, dS = \int_A pE_p \, dS \tag{28}$$

by noting that

$$-\int \psi dS = -\int \psi dS + \int \nabla_t \cdot (z'\psi \hat{e}_z) \, dS = \int z' \hat{e}_z \cdot \nabla_s \psi dS = -\int z'E_z dS$$

and similarly

$$-\int \psi dS = -\int pE_p \, dS.$$

Thus if $\hat{n}$ varies slowly over the aperture we have

$$\underline{p} = -\varepsilon_o \cdot \hat{n} \int z'E_z \, dS = -\varepsilon_o \hat{n} \int \psi dS \tag{28}$$

where E_z is the electrostatic field.

Returning to Equation 17 we find

$$I(z) = \frac{1}{2Z_o} \frac{\partial \phi_o}{\partial n} e^{ikz} \, (i\omega\mu_o \, \underline{m} \cdot \hat{e}_\phi + ik \, \underline{p} \cdot \hat{n}), \qquad z > b. \tag{29}$$

$$I(z) = \frac{e^{-ikz}}{2}\left(\frac{V_{eq}}{Z_o} - I_{eq}\right) \qquad z < -b$$

$$V(z) = -Z_c I(z). \qquad (34a)$$

Since $2kb << 1$ we can set

$$I(z=0+) = \frac{1}{2}\left(\frac{V_{eq}}{Z_c} + I_{eq}\right)$$

$$V(z=0+) = Z_c I(z=0+) \qquad (33b)$$

$$I(z=0-) = \frac{1}{2}\left(\frac{V_{eq}}{Z_c} - I_{eq}\right)$$

$$V(z=0-) = -Z_c I(z=0-) \qquad (34b)$$

with z=0+, z=0- meaning to the right and to the left of the small apertures respectively.

Figure 4 gives an interpretation of Equations 33 and 34, that is, V_{eq} and I_{eq} are voltage and current sources respectively acting at the location of the aperture and I(z), V(z) are the induced current and voltage waves propagating down the two branches of the infinite transmission line. If the transmission line is loaded as indicated in figure 5 we can apply standard transmission line theory to obtain

$$I(z) = \frac{1}{Z_c + Z_{TL}} \frac{\exp(ikz) + \rho_R \exp[ik(2L_1 - z)]}{1 - \rho_{OL}\,\rho_R \exp(2ikL_1)} V_{TL} \qquad z > 0$$

$$V(z) = \frac{Z_c}{Z_c + Z_{TL}} \frac{\exp(ikz) - \rho_R \exp[ik(2L_1 - z)]}{1 - \rho_{OL}\,\rho_R \exp(2ikL_1)} V_{TL} \qquad (35)$$

When $z < -b$, Equation 17 gives

$$I(z) = \frac{1}{2Z_o}\frac{\partial \phi_o}{\partial n} e^{-ikz}(i\omega\mu_o \underline{m} \cdot \hat{e}_\phi - ik\underline{p} \cdot \hat{n}) \qquad z < -b \tag{30}$$

and from Equation 11

$$V(z) = Z_c I(z) \qquad z > b$$

$$V(z) = -Z_c I(z) \qquad z < -b \tag{31}$$

where $Z_c = \sqrt{L/C}$.

For a coaxial cable, Equations 29 through 31 have been derived in reference 3. There is a sign difference between our equations and those in reference 3 because $\partial\phi_o/\partial n$ is a negative quantity.

If we define

$$V_{eq} \equiv i\omega\mu_o \frac{Z_c}{Z_o}\frac{\partial \phi_o}{\partial n}\underline{m} \cdot \hat{e}_\phi$$

$$I_{eq} \equiv i\omega \frac{\partial \phi_o}{\partial n}\underline{p} \cdot \hat{n} \tag{32}$$

then

$$I(z) = \frac{e^{ikz}}{2}\left(\frac{V_{eq}}{Z_o} + I_{eq}\right) \qquad z > b$$

$$V(z) = Z_c I(z) \tag{33a}$$

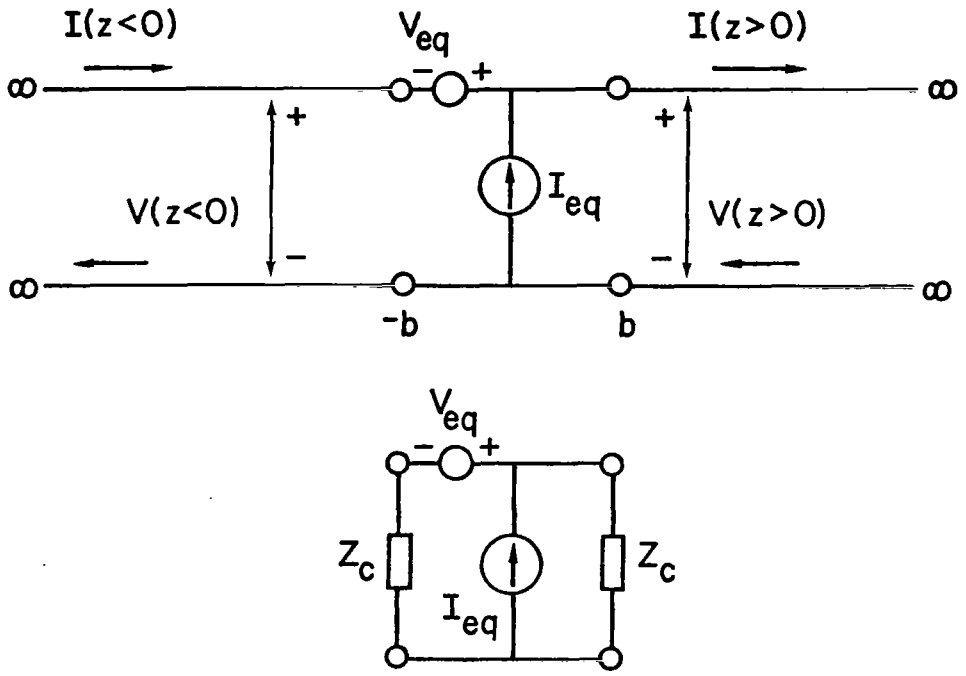

Figure 4. (a) Sign Conventions for Infinite Transmission Line
(b) Equivalent Network

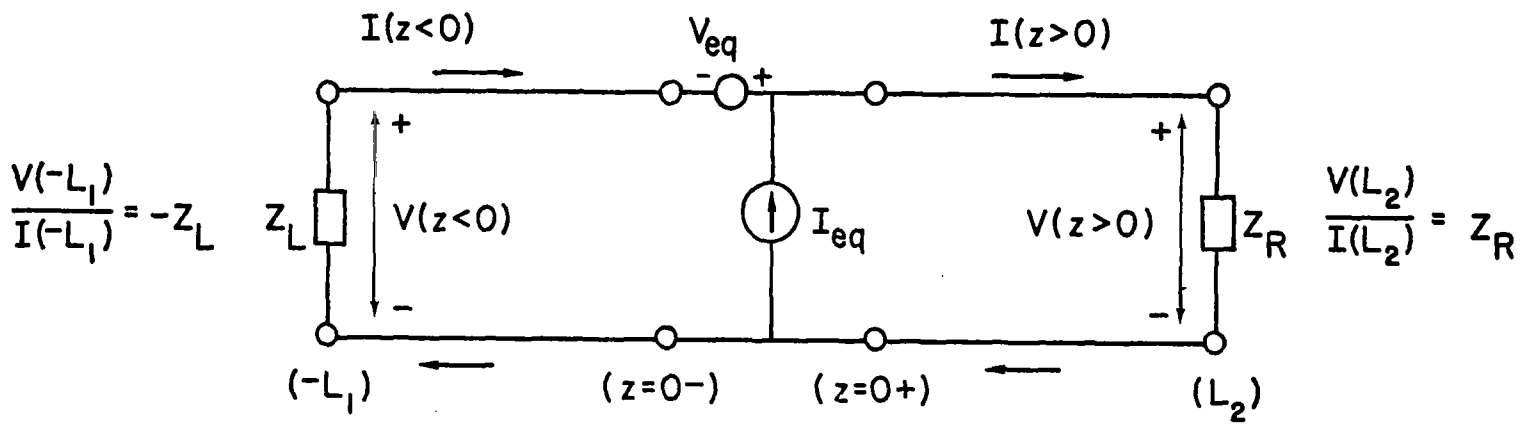

Figure 5. Sign Conventions for Currents and Voltages on the Two Branches of the Transmission Line

$$I(z) = \frac{1}{Z_c + Z_{TR}} \frac{\exp(-ikz) + \rho_L \exp[ik(2L_2+z)]}{1 - \rho_{OR}\,\rho_L \exp(2ikL_2)} V_{TR} \qquad z < 0$$

$$V(z) = \frac{-Z_c}{Z_c + Z_{TR}} \frac{\exp(-ikz) - \rho_L \exp[ik(2L_2+z)]}{1 - \rho_{OR}\,\rho_L \exp(2ikL_2)} V_{TR} \qquad (36)$$

where

$$\rho_R = \frac{Z_c - Z_R}{Z_c + Z_R}$$

$$\rho_L = \frac{Z_c - Z_L}{Z_c + Z_L} \qquad (37)$$

$$Z_{TL} = Z_c \frac{1 - \rho_L \exp(2ikL_2)}{1 + \rho_L \exp(2ikL_2)}$$

$$Z_{TR} = Z_c \frac{1 - \rho_R \exp(2ikL_1)}{1 + \rho_R \exp(2ikL_1)} \qquad (38)$$

$$\rho_{OL} = \frac{Z_c - Z_{TL}}{Z_c + Z_{TL}}$$

$$\rho_{OR} = \frac{Z_c - Z_{TR}}{Z_c + Z_{TR}} \qquad (39)$$

$$V_{TL} = V_{eq} + Z_{TL}\, I_{eq}$$

$$V_{TR} = V_{eq} - Z_{TR}\, I_{eq} \,. \qquad (40)$$

When L_1 and L_2 are infinite $\rho_R = \rho_L = \rho_{OR} = \rho_{OL} = 0$ and Equations 35 and 36 reduce to Equations 33 and 34. Notice

that for both branches the current is considered positive when it flows in the positive z-direction.

The calculation of I(z) and V(z) depends on the knowledge of V_{eq} and I_{eq} as defined by Equation 32. Z_c and $\partial\phi_o/\partial n$ are functions of the geometry of the waveguide with short-circuited apertures and $\underline{m}$ and $\underline{p}$ are given by Equations 25 and 28. As we mentioned earlier the aperture electric field can be obtained from knowledge of the short-circuited aperture current density and because of linearity we can write

$$\underline{m} = -\underline{\underline{\alpha}}_m^e \cdot \underline{H}_{s.c.}$$

$$\underline{p} = \varepsilon_o \alpha_e^e \underline{E}_{s.c.} \tag{41}$$

where $\underline{H}_{s.c.}$ and $\underline{E}_{s.c.}$ are the magnetic field and electric field averaged over the short-circuited aperture and calculated by solving the exterior interaction problem (with the aperture short-circuited). The exact magnetic and electric polarizations $\underline{\underline{a}}_m^e$, a_e^e depend on the full geometry of our problem. Because it is very difficult to calculate these quantities we make the following approximation. We define

$$\underline{m} = \underline{\underline{\alpha}}_m \cdot (-\underline{H}_{ext} + \underline{H}_{int})$$

$$\underline{p} = \varepsilon_o \alpha_e (\underline{E}_{ext} - \underline{E}_{int}) \tag{42}$$

where $\underline{H}_{ext}$, $\underline{E}_{ext}$ are equal to $\underline{H}_{s.c.}$, $\underline{E}_{s.c.}$ respectively, $\underline{H}_{int}$, $\underline{E}_{int}$ are the short-circuited fields for the interior problem, which, in our case, are the TEM fields, and $\underline{\underline{\alpha}}_m$, α_e are the polarizabilities for the interaction problem of a planar perfectly conducting screen with a (2b x 2a) aperture in it.

Before we discuss the validity of Equations 42 we explain the sign conventions. For a penetration problem through an aperture in a planar screen one defines the side where the source exists as the illuminated side and the other side where the transmitted fields exist as the shadow or transmission side. The dipole moment $\underline{p}$ in the shadow region is always parallel to the short-circuited electric field whereas the magnetic dipole moment $\underline{m}$ is always antiparallel to the short-circuited magnetic field. For calculations in the illuminated side $\underline{p}$ and $\underline{m}$ have opposite signs (fig. 6). As we will explain shortly, Equations 42 involve an external excitation through $\underline{E}_{ext}$, $\underline{H}_{ext}$ and an indirect internal excitation through $\underline{E}_{int}$, $\underline{H}_{int}$. By choosing a positive direction for the external and TEM fields as depicted in figure 7 we can now understand the signs in Equations 42. Thus in the shadow region (inside the waveguide) $\underline{p}_1$ due to the external excitation is equal to $\alpha_e \underline{E}_{ext}$ ($\alpha_e > 0$) and $\underline{p}_2$ due to the internal excitation in the illuminated side (still inside the waveguide) is parallel to $\underline{p}_1$ and equal to $-\alpha_e \underline{E}_{int}$, i.e., antiparallel to $\underline{E}_{int}$. Similarly $\underline{m}_1$ in the shadow region (inside the waveguide) due to the external excitation is equal to $-\underline{\underline{\alpha}}_m \cdot \underline{H}_{ext}$ ($\alpha_{mij} > 0$) and $\underline{m}_2$ due to the internal excitation in the illuminated side (still inside the waveguide) is equal to $\underline{\underline{\alpha}}_m \cdot \underline{H}_{int}$. In general $\underline{H}_{ext}$ has two nonzero orthogonal components whereas $\underline{H}_{int}$ only has one component in the ϕ-direction. In our case we are interested in $\underline{m} \cdot \hat{e}_\phi$, i.e., $-\alpha_{m\phi\phi}(H_{ext})_\phi - \alpha_{m\phi z}(H_{ext})_z$. As we will show at the end of this section, symmetry arguments require that $\alpha_{m\phi z} = 0$ and consequently we are left with $-\alpha_{m\phi\phi}(H_{ext})_\phi$, i.e., within the validity of our approximations the z-component of $\underline{H}_{ext}$ does not contribute.

The justification of Equations 42 goes as follows. If only a TEM internal excitation existed, the presence of the aperture would cause reflection of the TEM mode (and also generate higher order modes). Then $\underline{m}$ and $\underline{p}$ would be

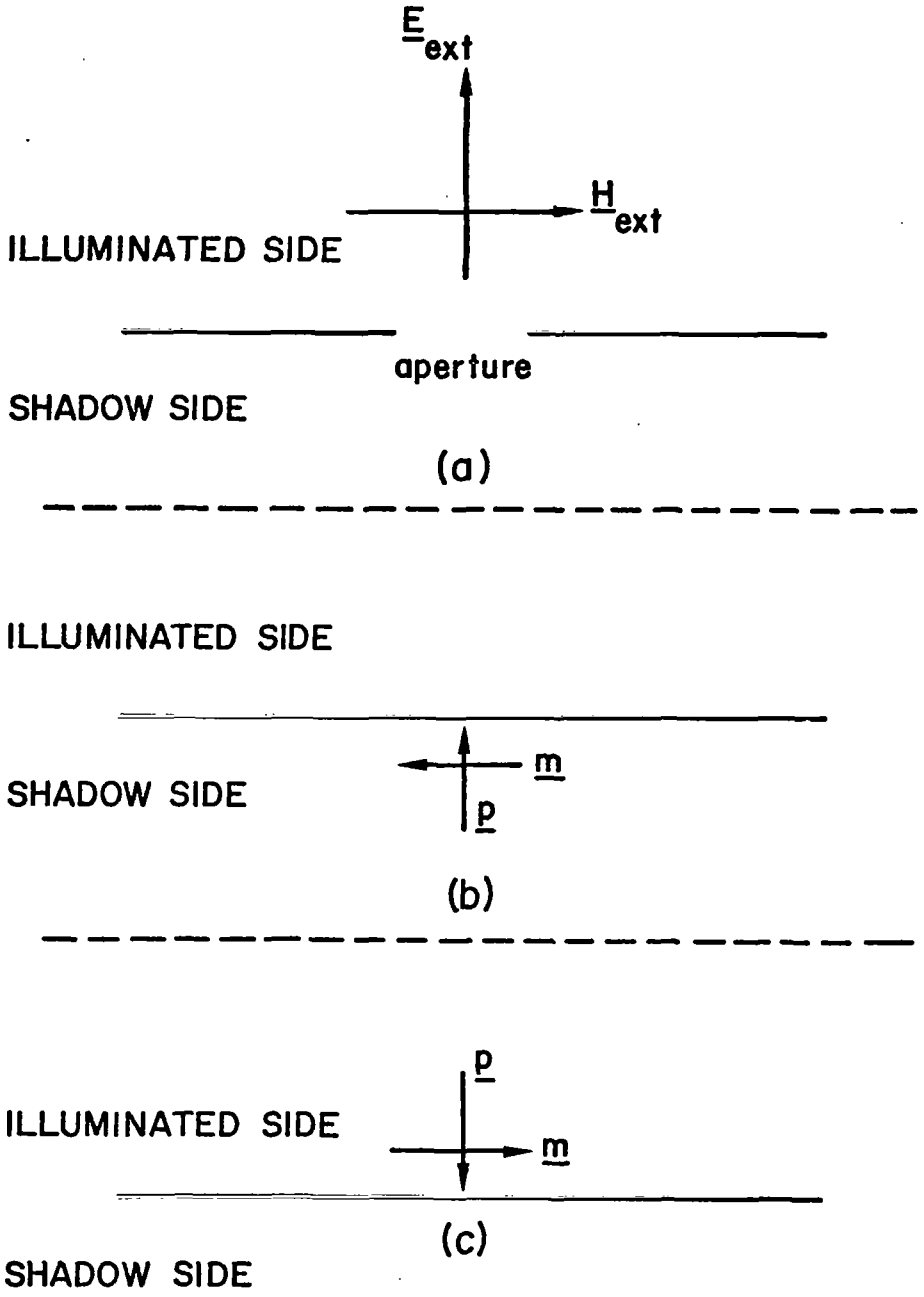

Figure 6. Directions for $\underline{m}$ and $\underline{p}$ for Calculations in the Shadow Region (b) and Illuminated Region (c)

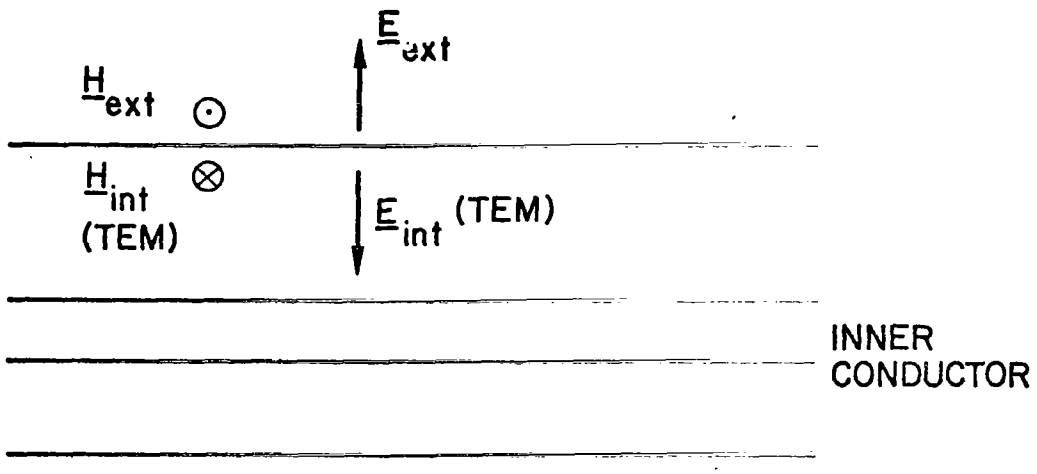

Figure 7. Positive Directions for External and Internal (TEM) Fields

proportional to $\underline{H}_{int}$ and $\underline{E}_{int}$ respectively. If the excitation is external then field penetration excites a TEM mode which is reflected by the loads and other apertures and again reflected by the discontinuity caused by the presence of the aperture. Thus the presence of $\underline{H}_{int}$, $\underline{E}_{int}$ in Equations 42 partially takes into account the interior geometry. (Notice that Equations 41 do not explicitly include the TEM fields. However, polarizabilities should be calculated by taking into account the exact geometry, interior and exterior, of the problem. From a boundary-value point of view the loads are geometrical structures with known electromagnetic proprerties and consequently α_m^e, α_e^e would contain their effect on the induced TEM fields.) The substitution of α_m^e and α_e^e by the planar polarizabilities is a good approximation if 2a is smaller than the distance between the aperture and any conductors inside the waveguide and also smaller than the radius of curvature at the aperture site (ref. 4). Our aperture width 2a is not smaller than the distances between the aperture and the nearby conductors. Notice, however, that using the planar polarizabilities will result in a larger amount of energy leaking into the wing cavity, that is, our calculation will provide an upper bound for the energy leakage and this is an acceptable result.

Equations 25 and 36 give the induced currents and voltages in terms of the equivalent sources, V_{eq} and I_{eq}. However, according to Equations 42 these sources contain the TEM fields, i.e., the induced currents and voltages. Thus we will have to rewrite Equations 35 and 36 in order to obtain the final expression for I(z) and V(z). A method that can readily be generalized to our real case involving periodic apertures is used in reference 3. The first step involves calculation of the equivalent lumped network for a small aperture. This

---

4. Latham, R. W., Small Holes in Cable Shields, Air Force Weapons Laboratory, Interaction Note 118, September 1972.

can be done by considering the internal excitation problem and defining

$$\underline{m} = \underline{\underline{\alpha}}_m \cdot \underline{H}_{int}$$

$$\underline{p} = -\varepsilon_o \alpha_e \underline{E}_{int} \tag{43}$$

Recalling Equations 2, 6, 7, 12 and 32 we find

$$V_{eq} = i\omega\mu_o \alpha_m \left(\frac{1}{N_o^2} \frac{\partial \phi_o}{\partial n}\right)^2 I$$

$$I_{eq} = -i\omega\varepsilon_o \alpha_e \left(\frac{\partial \phi_o}{\partial n}\right)^2 V \tag{44}$$

where

$$\alpha_m = \underline{\underline{\alpha}}_m : \hat{e}_\phi \, \hat{e}_\phi \tag{45}$$

and I and V are evaluated at the location of the aperture.

If we recall figure 4 we understand that the transmission line equations with internal excitation only are

$$\frac{dI}{dz} = i\omega CV + I_{eq} \, \delta(z)$$

$$\frac{dV}{dz} = i\omega LI + V_{eq} \, \delta(z) \tag{46}$$

because they satisfy the discontinuity conditions

$$I(0+) - I(0-) = I_{eq}$$

$$V(0+) - V(0-) = V_{eq}$$

dictated by figure 4.

Thus we can define

$$I_{eq} \equiv -i\omega C_a V$$

$$V_{eq} \equiv i\omega L_a I \tag{47}$$

and rewrite Equations 45 as

$$\frac{dI}{dz} = i\omega[c - C_a\delta(z)]\ V(z)$$

$$\frac{dV}{dz} = i\omega[L + L_a\delta(z)]\ I(z) \tag{48}$$

where

$$C_a = \varepsilon_o\alpha_e\left(\frac{\partial\phi_o}{\partial n}\right)^2$$

$$L_a = \mu_o\alpha_m\left(\frac{1}{N_o^2}\frac{\partial\phi_o}{\partial n}\right)^2. \tag{49}$$

The equivalent networks of the transmission line and the aperture are shown in figures 8a and 8b. (Notice that this representation of the aperture is purely reactive, i.e., does not account for radiation leakage through the aperture and into the exterior region. The reason for this is that our calculation for $\underline{m}$ and $\underline{p}$ makes $\alpha_{m\phi\phi}$ and α_e real. We could use $\underline{m}$ and $\underline{p}$ to calculate the radiated power into free space and introduce a resistive element to account for it. We will not attempt to do this because in the absence of radiation leakage into free space our calculation will again be an upper bound for the EMP energy leakage into the waveguide.)

If now an EMP interacts with the aircraft, we use Equation 42 to extend Equations 46 or 48

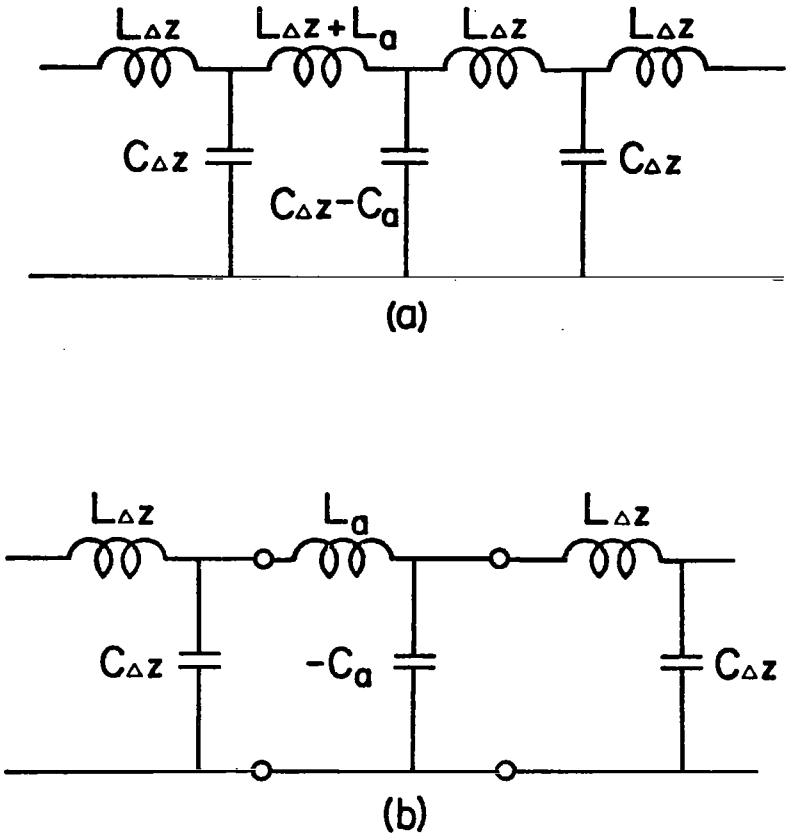

Figure 8. (a) Aperture Imbedded in the Network of the Transmission Line
(b) Network Representation of Aperture in the Transmission Line

$$\frac{dI}{dz} = i\omega[C - C_a\delta(z)]\ V(z) + I_{eq}\delta(z)$$

$$\frac{dV}{dz} = i\omega[L + L_a\delta(z)]\ I(z) + V_{eq}\delta(z) \qquad (50)$$

where from Equation 32

$$V_{eq} = -i\omega\mu_o \frac{Z_c}{Z_o} \frac{\partial\phi_o}{\partial n} (\underline{\underline{\alpha}}_m \cdot \underline{H}_{ext}) \cdot \hat{e}_\phi$$

$$I_{eq} = i\omega \frac{\partial\phi_o}{\partial n} \varepsilon_o \alpha_e \underline{E}_{ext} \cdot \hat{n} \ . \qquad (51)$$

Equations 50 assume the existence of only one small aperture. In our problem, however, we have a periodic configuration of apertures. As we see from figure 1 the apertures are trapezoidal and not of equal size. To simplify our calculation we will assume that all the apertures are rectangular and equal. The average width of the apertures will be the mean of the widths at intersections BB and AA. Again we tend to overestimate the amount of energy penetration by considering larger apertures than the ones that would result by averaging over the entire length of the wing.

If the ith aperture is located at $z = z_i$ we can rewrite Equation 50 as

$$\frac{dI}{dz} = i\omega\left[C - \sum_i C_a\delta(z - z_i)\right] V(z) + \sum_i I_{eq}\delta(z - z_i)$$

$$\frac{dV}{dz} = i\omega\left[L + \sum_a L_a\delta(z - z_i)\right] I(z) + \sum_i V_{eq}\delta(z - z_i) \qquad (52)$$

As shown in reference 3 one can expand the delta function in a cosine Fourier series over the interval -d to d and only keep the first term. Thus our final set of transmission line equations is

$$\frac{dI}{dz} = i\omega\left(C - \frac{C_a}{2d}\right) V(z) + \frac{I_{eq}(z)}{2d}$$

$$\frac{dV}{dz} = i\omega\left(L + \frac{L_a}{2d}\right) I(z) + \frac{V_{eq}(z)}{2d} \qquad (53)$$

where I_{eq} and V_{eq} are given by Equations 51 and C_a, L_a by Equations 49.

From Equations 53 we obtain

$$\frac{d^2I}{dz^2} + k_e^2 I = i\omega\left(C - \frac{C_a}{2d}\right)\frac{V_{eq}}{2d} + \frac{1}{2d}\frac{dI_{eq}}{dz} \qquad (54)$$

where

$$k_e^2 = \omega^2\left(C - \frac{C_a}{2d}\right)\left(L + \frac{L_a}{2d}\right) = k^2\left(1 - \frac{C_a}{2dC}\right)\left(1 + \frac{L_a}{2dL}\right). \qquad (55)$$

The particular solution of Equation 53 is

$$I_p(z) = \frac{1}{4ik_e d}\int_{-\infty}^{\infty}\left[i\omega\left(C - \frac{C_a}{2d}\right)V_{eq} + \frac{dI_{eq}}{dz'}\right] e^{ik_e|z-z'|}\, dz'$$

or after some manipulations

$$I_p(z) = I^- e^{-ik_e z} \qquad z < L_1$$

$$I_p(z) = I_1(L_1, z)\, e^{ik_e z} + I_2(z, L_2)\, e^{-ik_e z} \qquad L_1 < z < L_2$$

$$I_p(z) = I^+ e^{ik_e z} \qquad z > L_2 \qquad (56)$$

where

$$I_1(L_1,z) = \frac{1}{4Z_{ec}d}\int_{L_1}^{z}\left[V_{eq}(z') + Z_{ec}\, I_{eq}(z')\right] e^{-ik_e z'}\, dz'$$

$$I^+ = I_1(L_1,L_2)$$

$$I_2(z,L_2) = \frac{1}{4Z_{ec}d}\int_{z}^{L_2}\left[V_{eq}(z') - Z_{ec}\, I_{eq}(z')\right] e^{ik_e z'}\, dz'$$

$$I^- = I_2(L_1,L_2) \qquad (57)$$

and

$$Z_{ec} = \left(\frac{L + L_a/2d}{C - C_a/2d}\right)^{1/2}. \qquad (58)$$

In deriving Equations 57 we have assumed that the aperture configuration extends from $z = L_1$ to $z = L_2$ and that $I_{eq}(z)$ and $V_{eq}(z)$ are zero for $z < L_1$ and $z > L_2$. Using the first of Equation 53 we can obtain the particular solution for V(z).

If the transmission line is loaded at $z = 0$ and $z = L_3$ with impedances Z_L and Z_R respectively, the total current solution (particular + complementary) is

$$I(z) = -\frac{\rho_R I^+ + e^{-2ik_e L_3}\, I^-}{\rho_R\rho_L - e^{-2ik_e L_3}}\left(\rho_L\, e^{ik_e z} + e^{-ik_e z}\right), \quad z < L_1 \qquad (59)$$

$$I(z) = \frac{1}{\rho_R\rho_L - e^{-2ik_eL_3}} \left\{ \left[-\rho_L \left(I^- e^{-2ik_eL_3} + \rho_R I^+ \right) + \left(\rho_R\rho_L - e^{-2ik_eL_3} \right) I_1(L_1,z) \right] e^{ik_ez} + \left[-\rho_R \left(I^+ + \rho_L I^- \right) + \left(\rho_R\rho_L - e^{-2ik_eL_3} \right) I_2(z,L_2) \right] e^{-ik_ez} \right\} \qquad L_1 < z < L_2$$

$$I(z) = -\frac{I^+ + \rho_L I^-}{\rho_R\rho_L - e^{-2ik_eL_3}} e^{ik_e(z-2L_3)} + \rho_R e^{-ik_ez} \qquad z > L_2 \qquad (59)$$

where

$$\rho_L = \frac{Z_{ce} - Z_L}{Z_{ce} + Z_L}$$

$$\rho_R = \frac{Z_{ce} - Z_R}{Z_{ce} + Z_R} \qquad (60)$$

$$Z_{ce} = \left(\frac{L + L_a/2d}{C - C_a/2d} \right)^{1/2} \qquad (58)$$

k_e is given by Equation 55, C_a, L_a by Equation 49 and V_{eq}, I_{eq} by Equation 51. (Notice that we have set $V(0)/I(0) = -Z_L$ and $V(L_3)/I(L_3) = Z_R$ because of the conventions in figure 5.

To find V(z) we use the first of Equations 53 and notice that

$$\frac{dI_1(L_1,z)}{dz} e^{ik_ez} + \frac{dI_2(z,L_2)}{dz} e^{-ik_ez} = \frac{I_{eq}}{2d} \qquad (61)$$

Consequently the voltage can be obtained by multiplying the current waveforms that propagate in the ±z-directions by $\pm Z_{ec}$.

In order to explicitly exhibit the dependence of the induced current and voltage on the parameters of the problem, we obtain an upper bound for the simple case $Z_R = Z_L = Z_{ce}$, i.e., when the equivalent transmission line is matched. (In general, similar bounds can be obtained through Equations 59). Thus we recall Equations 56

$$I_p(z) = I^- e^{-ik_e z} \qquad z < L_1$$
$$V_p(z) = -Z_{ec} I_p(z)$$

$$I_p(z) = I^+ e^{ik_e z} \qquad z > L_2$$
$$V_p(z) = Z_{ec} I_p(z)$$

where

$$I^- = \frac{1}{4Z_{ec}^d} \int_{L_1}^{L_2} [V_{eq}(z') - Z_{ec} I_{eq}(z')] e^{ik_e z'} dz'$$

$$I^+ = \frac{1}{4Z_{ec}^d} \int_{L_1}^{L_2} [V_{eq}(z') + Z_{ec} I_{eq}(z')] e^{-ik_e z'} dz'.$$

We can now write

$$I = \frac{1}{4Z_{ec}d} \int_{L_1}^{L_2} [V_{eq}(z') \pm Z_{ec} I_{eq}(z')] e^{\mp ik_e(z'-z)} dz'$$

$$< \frac{1}{4Z_{ec}d} \int_{L_1}^{L_2} |V_{eq}(z') \pm Z_{ec} I_{eq}(z')| dz'.$$

$$I < \frac{1}{4Z_{ec}d} \int_{L_1}^{L_2} \left\{ |V_{eq}(z')| + |Z_{ec} I_{eq}(z')| \right\} dz'$$

$$= \frac{L_w}{2(2d)} \left\{ \frac{\tilde{V}_{eq}}{Z_{ec}} + \tilde{I}_{eq} \right\} \qquad (62)$$

where $L_w = L_2 - L_1$ and $(L_2 - L_1)\ \tilde{f} \equiv \int_{L_1}^{L_2} |f(z')| dz'$. The driving terms V_{eq} and I_{eq} are given by Equation 51. $\underline{H}_{ext}$ and $\underline{E}_{ext}$ are the magnetic and electric fields on the short-circuited aperture configuration and are obtained by solving the external interaction problem. By modeling the interior of the wing cavity in a certain way we can also calculate $\partial\phi_o/\partial n$ and Z_c. This will be done in the next section. Finally the knowledge of $\hat{e}_\phi \cdot \underline{\underline{\alpha}}_m \cdot \hat{e}_\phi = \alpha_{m\phi\phi}$, $\hat{e}_\phi \cdot \underline{\underline{\alpha}}_m \cdot \hat{e}_z = \alpha_{m\phi z}$ and α_e is required. The first and second quantities result from considering $\underline{H}_{ext}$ in the ϕ- and z-direction respectively and approximate formulas for their calculation are developed in appendix B. The third quantity $\alpha_{m\phi z}$ is zero for the following reason. We have, by definition,

$$\underline{m} = -\int \underline{r}_s \, \hat{n} \cdot \underline{H} \, ds'$$

and

$$\underline{m} = -\underline{\underline{\alpha}}_m \cdot \underline{H}_{ext}.$$

If we consider a rectangular aperture in a planar screen (fig. 9) then

$$-\underline{m} \cdot \hat{e}_x = \alpha_{mxx}(H_{ext})_x + \alpha_{mxz}(H_{ext})_z$$

and

$$\underline{m} \cdot \hat{e}_x = -\int_{-a}^{a} \int_{-b}^{b} x' \, H_n \, dx'dz'.$$

For an $\underline{H}_{ext}$ in the z-direction the normal component of the total $\underline{H}$ in the aperture is antisymmetric with respect to the center of the aperture in the z-direction and consequently the integral over z vanishes. Thus $\alpha_{mzx} = 0$. In our case we have a periodic configuration of rectangular apertures but the normal component of $\underline{H}$ in any aperture is still antisymmetric with respect to the center of the aperture in the z-direction and α_{mzx} is zero. (Actually because our array of apertures is finite the antisymmetry property breaks down near the end apertures but the contribution from α_{mzx} of the end apertures should be small compared to the excess energy leakage due to a number of overestimations we made in our previous calculations.)

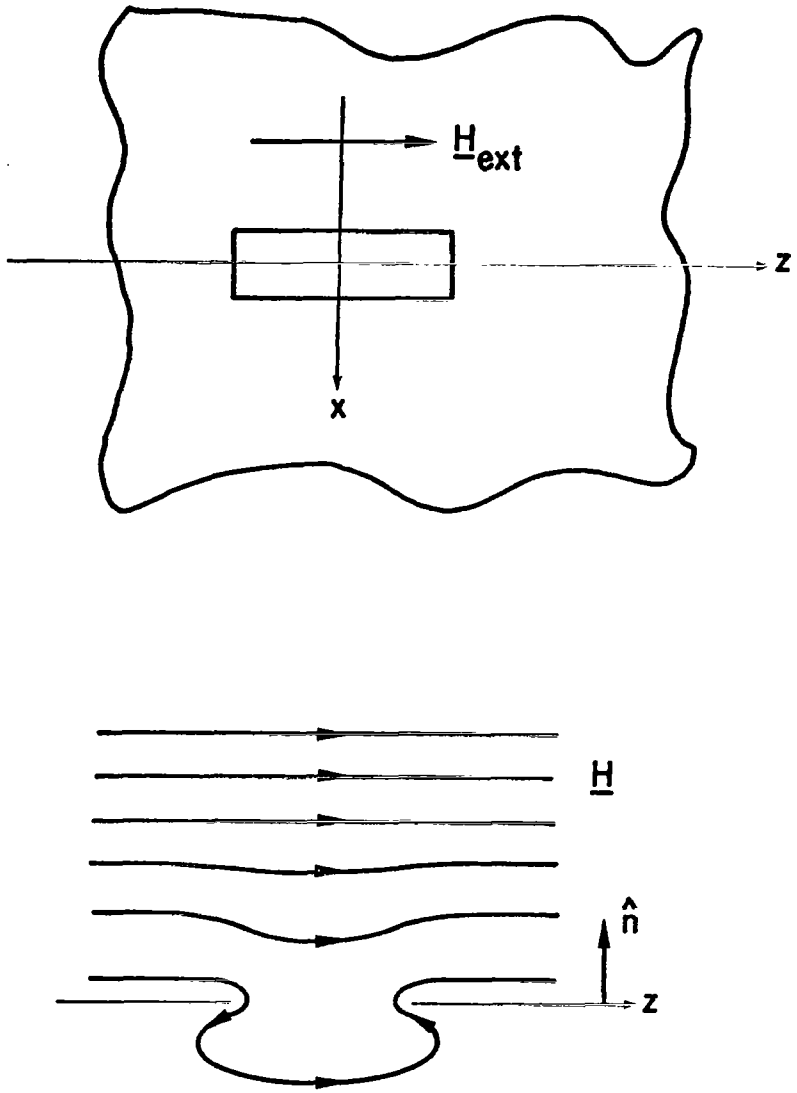

Figure 9. Geometry Showing the Antisymmetry Property
$H_n(z) = -H_n(-z)$

SECTION III

CALCULATIONS OF TEM PARAMETERS AND CURRENT ON THE CABLES

1. TEM PARAMETERS

In order to calculate the TEM parameters, the wing cavity shown in figure 1 with shielded apertures will be modeled as a perfectly conducting cylindrical tube of triangular cross section with the pneumatic duct as the only inner conductor. The actual wing cavity does not have a constant cross section but again allowing for overestimation of the EMP energy leakage we will assume that our cylindrical tube has a cross section equal to an appropriate average of the true cross sections at interesections B-B and A-A, i.e., an average weighted more by the larger cross section B-B. (More energy is expected to leak into a large empty cavity than a small empty one through the same aperture assuming that all dimensions are much smaller than the wavelength of the electromagnetic wave. Also the pneumatic duct in cross section B-B is closer to the leading edge of the wing and depending on the direction and polarization of the incident EMP the induced current density and charge density can assume large values at the leading edge and close to it.)

First we calculate an approximate expression for the potential ϕ_o satisfying Laplace's equation and $\phi_o = 0$, $\phi_o = 1$ on the walls and the inner conductor respectively. If we consider a line source, with a charge per unit length equal to Q, located at the center of the pneumatic duct, then the equipotential curves around the line source and close to it are approximately circles. Thus we will set the potential ϕ_o at $x = x_c = x_o - a_D$, $y = y_c = y_o$ equal to unity, where x_o, y_o are the coordinates of the center of the pneumatic duct

(fig. 10). The potential $\phi_o(x,y)$ will be found approximately by using eight images as shown in figure 11. These eight charges are chosen such that $\phi_o = 0$ on the hypotenuse and $\phi_o \approx 0$ on the other two sides. The potential due to the above charges is

$$\phi_o = \frac{Q}{2\pi\epsilon} \ln \frac{N(x,y;\ x_o,y_o)}{D(x,y;\ x_o,y_o)} \tag{63}$$

where

$$N(x,y;\ x_o,y_o) = R(x_o,y_o)\ R(-x_o,-y_o)$$
$$R[x'(x_o,-y_o),\ y'(x_o,-y_o)]\ R[x'(-x_o,y_o),\ y'(-x_o,y_o)]$$

$$D(x,y;\ x_o,y_o) = R(-x_o,y_o)\ R(x_o,-y_o)$$
$$R[x'(x_o,y_o),\ y'(x_o,y_o)]\ R[x'(-x_o,-y_o),\ y'(-x_o,-y_o)] \tag{64}$$

$$R(x_i,y_i) = \left[(x - x_i)^2 + (y - y_i)^2\right]^{1/2} \tag{65}$$

$$x'(x_i,y_i) = x_i \cos 2\alpha + (\ell - y_i) \sin 2\alpha$$

$$y'(x_i,y_i) = -y_i \cos 2\alpha + 2\ell \cos^2 \alpha - x_i \sin 2\alpha \tag{66}$$

By requiring that $\phi_o(x_o - a_D,\ y_o) = 1$ we determine the unknown Q and obtain

$$\phi_o = \left[\ln \frac{N(x,y;\ x_o,y_o)}{D(x,y;\ x_o,y_o)}\right] \Big/ \left[\ln \frac{N(x_c,y_c;\ x_o,y_o)}{D(x_c,y_c;\ x_o,y_o)}\right] \tag{67}$$

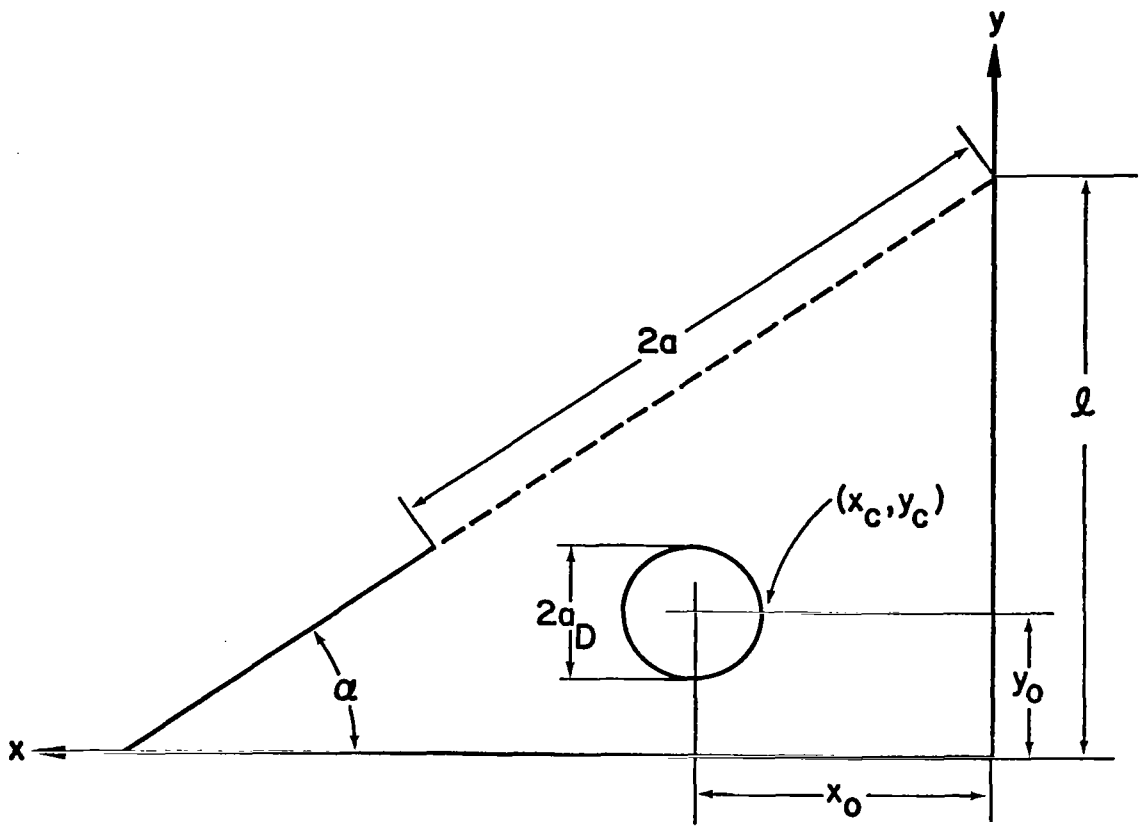

Figure 10. The Wing Cavity Cross Section Modeled as a Triangle

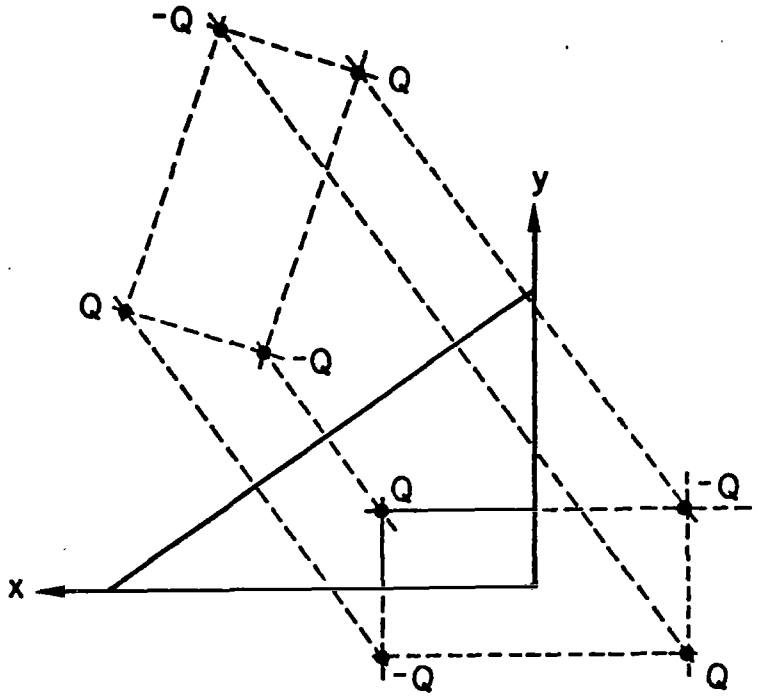

Figure 11. The Eight Charges Used in the Calculation of the Potential Function

With the aid of Equation 67 we will now calculate N_o^2 given by the first integral in Equation 9. Assuming that the pneumatic duct surface is equipotential (which is approximately true) we have

$$-\nabla\phi_o \cdot \hat{e}_\rho \approx -\nabla \frac{\ell n[R(x_o,y_o)]}{\ell n(Nc/Dc)} \cdot \hat{e}_\rho \Big|_{x_c,y_c}$$

$$= - \frac{1}{R(x_o,y_o)\ \ell n(N_c/D_c)} \Big|_{x_c,y_c}$$

$$\approx - \frac{1}{a_D \ell n(N_c/D_c)} = \frac{1}{a_D \ell n(D_c/N_c)} \qquad (68)$$

and

$$N_o^2 = \frac{2\pi}{\ell n(D_c/N_c)} \qquad (69)$$

where

$$N_c = N(x_c,y_c;\ x_o,y_o),\ D_c = D(x_c,y_c;\ x_o,y_o). \qquad (70)$$

Combining Equations 60 and 12 we obtain

$$L = \mu_o \frac{\ell n(D_c/N_c)}{2\pi}$$

$$C = \epsilon_o \frac{2\pi}{\ell n(D_c/N_c)}$$

$$Z_c = Z_o \frac{\ell n(D_c/N_c)}{2\pi}$$

$$Z_o = (\mu_o/\epsilon_o)^{1/2} \qquad (71)$$

Next we calculate $\partial\phi_o/\partial n$ on the hypotenuse. Referring to figure 12 we obtain

$$\frac{\partial\phi_o}{\partial n} = 2K \left[\frac{\cos\,\theta(x_o,y_o)}{R(x_o,y_o)} + \frac{\cos\,\theta(-x_o,-y_o)}{R(-x_o,-y_o)} - \frac{\cos\,\theta(-x_o,y_o)}{R(-x_o,y_o)} - \frac{\cos\,\theta(x_o,-y_o)}{R(x_o,-y_o)} \right] \tag{72}$$

where

$$K = \left[\ell n \frac{N(x_c,y_c;\, x_o,y_o)}{D(x_c,y_c;\, x_o,y_o)} \right]^{-1} = -\frac{N_o^2}{2\pi} \quad (x_c = x_o - a_D,\ y_c = y_o) \tag{73}$$

$$\cos\,\theta(x_i,y_i) = \hat{n} \cdot \hat{e}_{R_i} = (\sin\alpha\,\hat{e}_x + \cos\alpha\,\hat{e}_y) \cdot \left(\frac{-x_i + x}{R_i}\,\hat{e}_x + \frac{-y_i + y}{R_i}\,\hat{e}_y \right)$$

$$= \frac{(x - x_i)\sin\alpha + (y - y_i)\cos\alpha}{R_i}$$

$$= \frac{(\ell - y_i)\cos\alpha - x_i \sin\alpha}{R_i} \tag{74}$$

$$R_i = R(x_i,y_i) = [(x - x_i)^2 + (y - y_i)^2]^{1/2}$$

$$y = \ell - x\tan\alpha \tag{75}$$

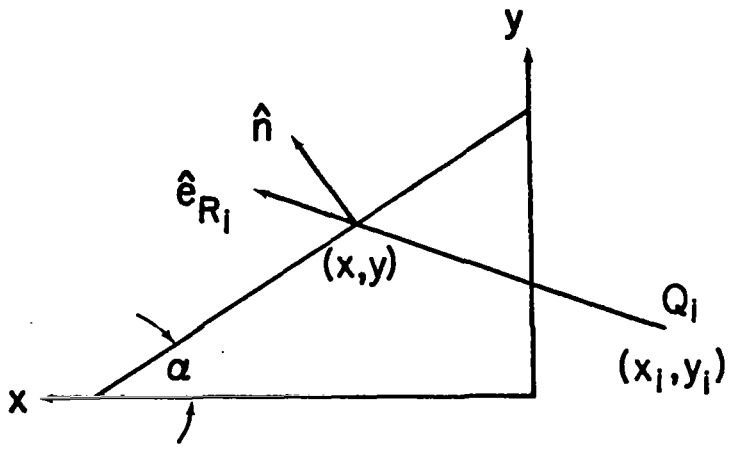

Figure 12. Geometry Appropriate for the Calculation of $\partial\phi_o/\partial n$ on the Hypotenuse

Equation 72 calculates $\partial\phi_o/\partial n$ at a point along the aperture. If we recall Equations 11 we understand that the subsequent formulas were derived under the assumption that $\partial\phi_o/\partial n$ varied slowly over the aperture. In reality, i.e., in the present case, this assumption is not valid because actually $\partial\phi_o/\partial n$ varies considerably over the aperture. For the model of the cross section of the wing cavity, which we will introduce in the next section, the maximum $-\partial\phi_o/\partial n$ is 5.04 and the average (over the aperture) is 1.87. The true $\partial\phi_o/\partial n$ that should be used in Equation 51 is

$$(\partial\phi_o/\partial n)_T = \frac{\int_c E_z(\partial\phi_o/\partial n)\,dc}{\int_c E_z\,dc} \tag{76}$$

as we can see from Equations 11. For a planar rectangular aperture with a uniform $\underline{H}_{ext}$, E_z varies slowly except near the edges where it goes to zero (in a direction perpendicular to z). Also E_z does not change sign over the aperture. In the present case $(H_{ext})_\phi$ or equivalently J_z (the induced short-circuited current density on the wing) varies over the aperture but E_z still vanishes at the edges and does not change sign; its maximum, however, will be shifted from the center. If E_z does not change sign, Equation 76 shows that

$$\left(-\frac{\partial\phi_o}{\partial n}\right)_T < \left(-\frac{\partial\phi_o}{\partial n}\right)_{max}.$$

Depending on the particular configuration $-(\partial\phi_o/\partial n)_T$ can be smaller or larger than $(-\partial\phi_o/\partial n)_{av} = (1/2a)\int_c(-\partial\phi_o/\partial n)\,dc$ where 2a is the width of the aperture (in the ϕ-direction). If $\partial\phi_o/\partial n$ peaked sharply in such a way that we could replace $\partial\phi_o/\partial n$ by $A + B\delta(c - c_o)$, where $A + B/2a = (\partial\phi_o/\partial n)_{av}$, then Equation 76 would give

$$\left(\frac{\partial\phi_o}{\partial n}\right)_T = A + \frac{(E_z)_o\, B}{\int_c E_z dc} = A + \frac{(E_z/E_m)_o\ (B/2a)}{\int_c (E_z/E_m)\,(dc/2a)}$$

where E_m is the maximum E_z and $(E_z)_o$ is E_z evaluated at $c = c_o$ where $-\partial\phi_o/\partial n$ is maximum. Notice that $(E_z/E_m)_o \leq 1$ and $\int_c (E_z/E_m)(dc/2a) < 1$. Thus $(\partial\phi_o/\partial n)_T$ can, as we mentioned earlier, be smaller or larger than $A + B/2a = (\partial\phi_o/\partial n)_{av}$. If E_z peaked at the same position as $-\partial\phi_o/\partial n$ then $(-\partial\phi_o/\partial n)_T$ would be smaller than $(-\partial\phi_o/\partial n)_{av}$. However, as we mentioned earlier, the position for E_m is shifted from the center and depending on its exact location $(-\partial\phi_o/\partial n)_T$ can be larger than $(-\partial\phi_o/\partial n)_{av}$. We will assume that $(-\partial\phi_o/\partial n)_{av} < (-\partial\phi_o/\partial n)_T$ and

$$\left(\frac{\partial\phi_o}{\partial n}\right)_T = \frac{1}{2}\left[\left(\frac{\partial\phi_o}{\partial n}\right)_{max} + \left(\frac{\partial\phi_o}{\partial n}\right)_{av}\right] \tag{77}$$

as the value for $\partial\phi_o/\partial n$ to be used in Equation 51. For completeness we give the formula for $(\partial\phi_o/\partial n)_{av}$

$$\left(\frac{\partial\phi_o}{\partial n}\right)_{av} = -\frac{N_o^2}{2\pi a}\sum_{i=1}^{4}\epsilon_i\left(\tan^{-1}\frac{2a - x_i\cos\alpha - (\ell - y_i)\sin\alpha}{|x_i\sin\alpha - (\ell - y_i)\cos\alpha|}\right.$$

$$\left. + \tan^{-1}\frac{x_i\cos\alpha + (\ell - y_i)\sin\alpha}{|x_i\sin\alpha - (\ell - y_i)\cos\alpha|}\right) \tag{78}$$

where $(x_1,y_1 = x_o,y_o)$, $(x_2,y_2 = -x_o,-y_o)$, $(x_3,y_3 = -x_o,y_o)$ $(x_4,y_4 = x_o,-y_o)$, $\epsilon_1 = \epsilon_2 = 1$, $\epsilon_3 = \epsilon_4 = -1$, 2a is the aperture width and N_o^2 is given by Equation 69.

2. CURRENT ON CABLES

In order to calculate the current induced on the cables we assume that they are so closely spaced together that they form a conducting wall which coincides with the partition wall. Then the current density induced on this wall is equal to $\hat{n} \times \underline{H}$ where $\underline{H}$ is the total magnetic field on the wall. Assuming that only the TEM mode contributes, we can calculate $\hat{n} \times \underline{H}$ using Equation 2, i.e.,

$$\hat{n} \times \underline{H} = \alpha_o(z)\ \hat{n} \times (\hat{e}_z \times \nabla_t \phi_o)$$

$$= \alpha_o(z)\ \frac{\partial \phi_o}{\partial x}\ \hat{e}_z = \frac{I(z)}{N_o^2}\ \frac{\partial \phi_o}{\partial x}\ \hat{e}_z \qquad (79)$$

Then the current induced on a cable will be

$$I_c \approx \frac{I(z)}{N_o^2}\ \frac{\partial \phi_o}{\partial x}\ (2a_c) \qquad (80)$$

where a_c is the radius of a cable.

We have already calculated I(z) in section II (Equation 58) and N_o^2 is given by Equation 69. In order to calculate $\partial\phi_o/\partial x$ we can use four charges (fig. 13) or twelve (fig. 14). Both cases make $\phi_o = 0$ (exactly) on the partition wall. With four charges we obtain a larger $\partial\phi_o/\partial x$ than with twelve charges, i.e., we overestimate the current I_c induced on the cables. We will give both formulas.

a. Four Charges

$$\frac{\partial \phi_o}{\partial x} = -\frac{N_o^2}{\pi}\left[\frac{1}{R^2(x_o, y_o)} - \frac{1}{R^2(x_o, -y_o)}\right] \qquad (81)$$

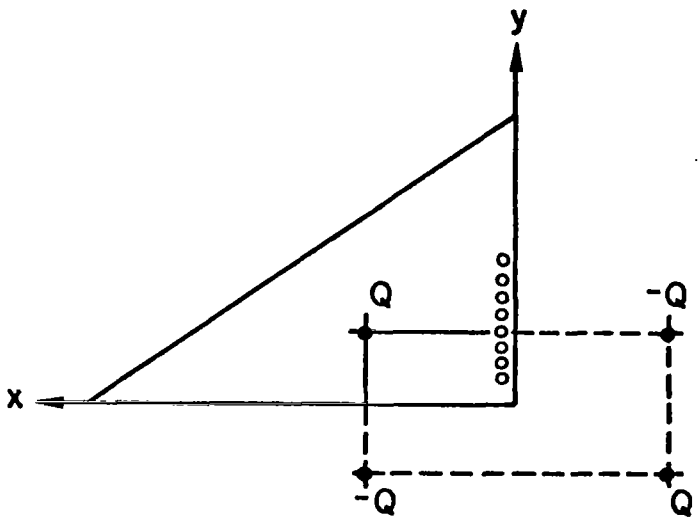

Figure 13. Geometry if Four Charges are Used in the Calculation of $\partial\phi_o/\partial n$ on the Partition Wall

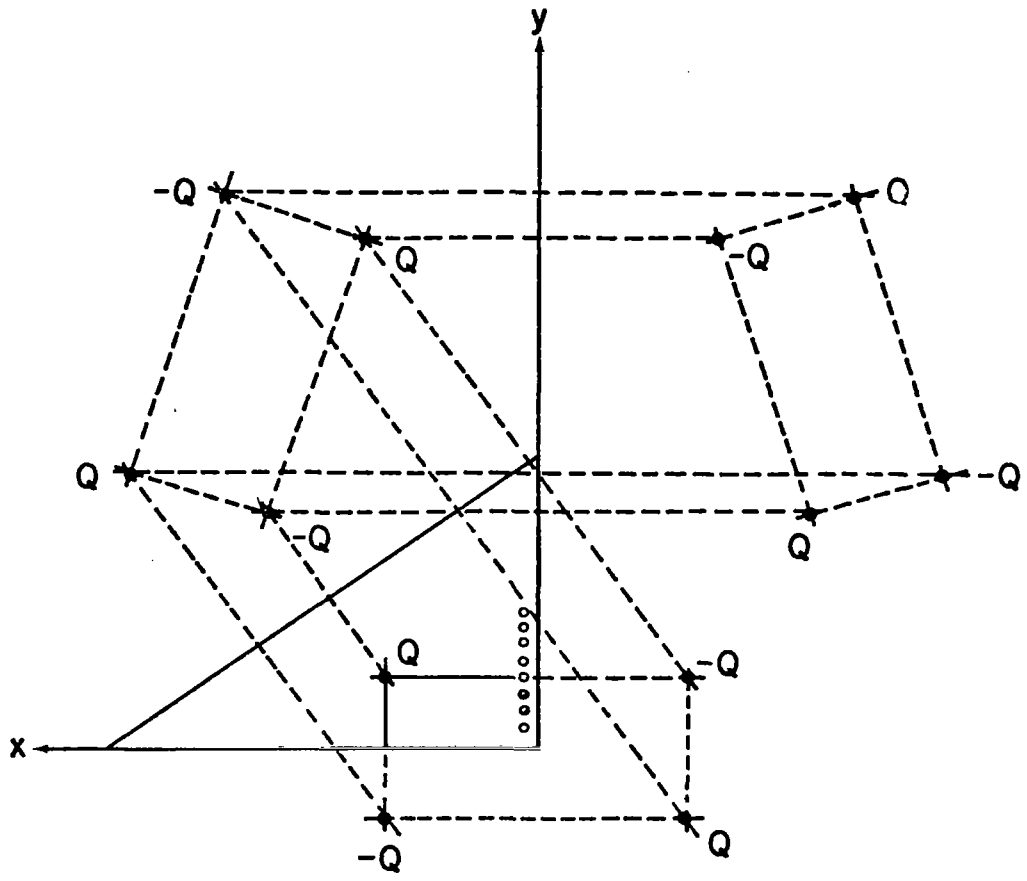

Figure 14. Geometry if Twelve Charges are Used for the Calculation $\partial\phi_o/\partial n$ on the Partition Wall

where K is given by Equation 73,

$$R^2(x_o, \pm y_o) = x_o^2 + (y \mp y_o)^2 \tag{82}$$

and y is the y-coordinate of a point on the partition wall.

b. Twelve Charges

$$\frac{\partial \phi_o}{\partial x} = -\frac{N_o^2}{\pi}\left[\frac{1}{R^2(x_o, y_o)} - \frac{1}{R^2(x_o, -y_o)}\right] + 2K\left\{\frac{x'(x_o, y_o)}{R^2[(x'(x_o, -y_o),\ y'(x_o, -y_o)]}\right.$$

$$+ \frac{x'(-x_o, y_o)}{R^2[x'(-x_o, y_o),\ y'(-x_o, y_o)]}$$

$$- \frac{x'(x_o, y_o)}{R^2 x'(x_o, y_o),\ y'(x_o, y_o)]}$$

$$\left. - \frac{x'(-x_o, -y_o)}{R^2[x'(-x_o, -y_o),\ y'(-x_o, -y_o)]}\right\} \tag{83}$$

where K is given by Equation 73, $x'(x_i, y_i)$ and $y'(x_i, y_i)$ by Equation 66,

$$R^2(x_i, y_i) = x_i^2 + (y - y_i)^2 \tag{84}$$

and y is the y-coordinate of a point on the partition wall.

SECTION IV

SUMMARY AND NUMERICAL EXAMPLE

In this report we have considered the problem of EMP penetration through dielectric skin panels covering part of the leading edge of the wings of an aircraft (fig. 1). In order to assess the effect of energy leakage into the wing we calculated the current and voltage induced on the pneumatic duct (this voltage is the potential difference between the duct and the metallic wall of the wing) and the current induced on the unshielded cables positioned in front of the partition wall (fig. 1). In order to perform these calculations analytically, we modeled the leading edge of the wing backed by the partition wall as a cylindrical tube of triangular cross section with a periodic array of rectangular apertures on its top side (fig. 15). (For simplicity the dielectric skin panels were replaced by air and as a result, our calculations overestimate the amount of energy leakage.) The pneumatic duct and the triangular tube, with the apertures short circuited, formed a structure that could support a TEM mode which, due to low frequencies comprising the bulk of the EMP spectrum, was the dominant mode to be excited. Thus we were able to neglect higher order modes and derive an equivalent transmission line to describe the behavior of the pneumatic duct. For this calculation we ignored the presence of any other metallic objects housed in the wing cavity (including the unshielded cables). Once we determined the TEM electromagnetic field we calculated the current induced on the unshielded cables by assuming that they were sufficiently close to each other to form a wall (see section III). Figure 15 depicts the equivalent transmission line for the pneumatic duct. We have calculated the induced current on the duct by assuming two general loads,

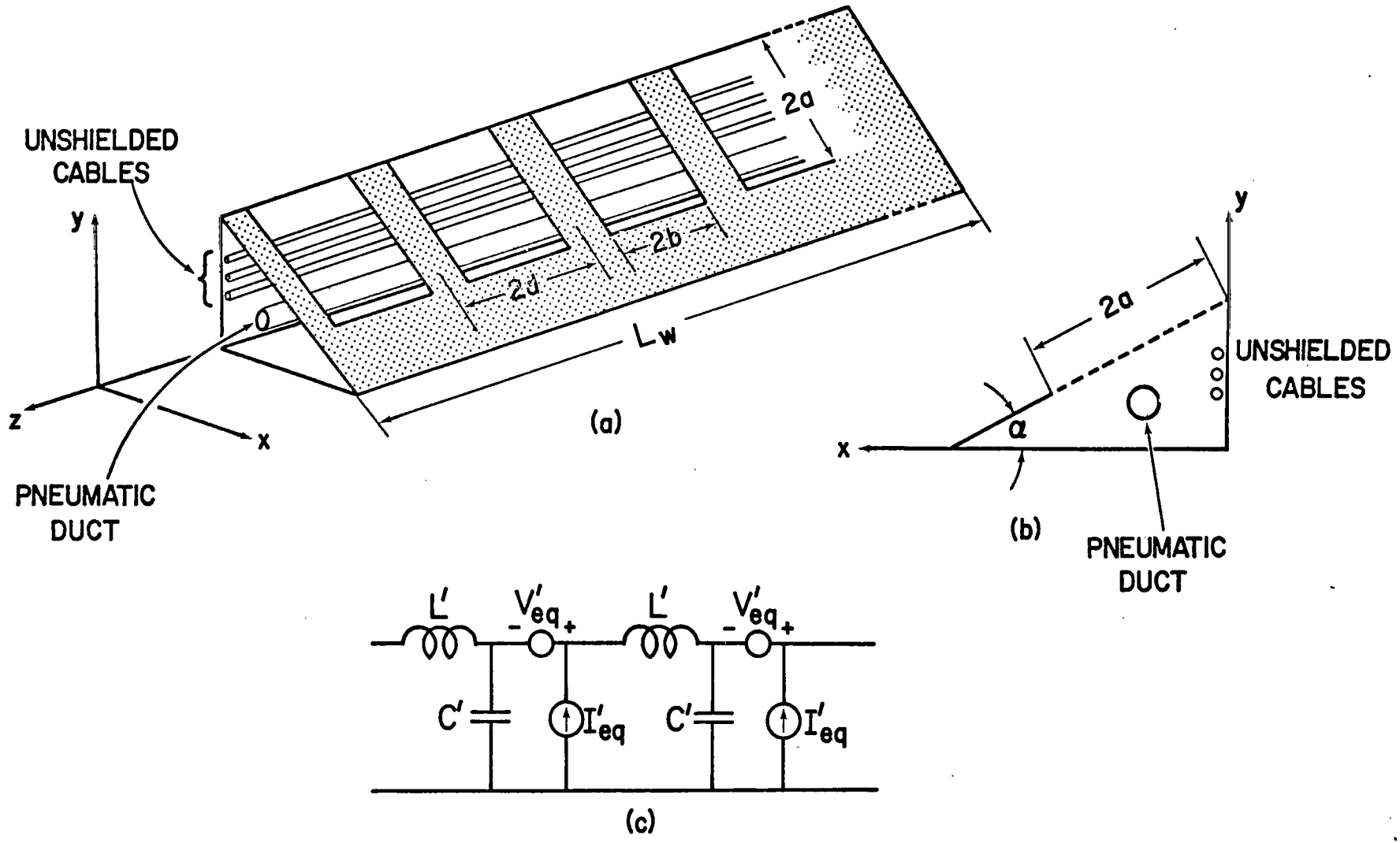

Figure 15. (a) and (b) The Edge of the Wing Modeled as a Cylindrical Tube with a Triangular Cross Section and a Periodic Array of Rectangular Apertures on it. (c) The Equivalent Circuit for the Pneumatic Duct

Z_L, Z_R terminating the transmission line on the left and right sides respectively (Equations 59). The voltage can be obtained by multiplying the current waveforms that propagate in the ±z-directions by $\pm Z_{ec}$ where $Z_{ec} = (L'/C')$ is the characteristic impedance of the transmission line. The parameters shown in figure 15 are given by the following formulas.

$$L' = L + \frac{L_a}{2d} \quad \text{(Henry/m)}, \qquad C' = C - \frac{C_a}{2d} \quad \text{(Farad/m)}$$

$$V'_{eq} = - \frac{i\omega\mu_o\alpha_m}{2d} \frac{Z_c}{Z_o} \frac{\partial\phi}{\partial n} J_z(z) \quad \text{(volts/m)}$$

$$I'_{eq} = \frac{i\omega\alpha_e}{2d} \frac{\partial\phi}{\partial n} \sigma(z) \quad \text{(Amps/m)}$$

$$L = \frac{\mu_o}{N_o^2} \quad \text{(Henry/m)}, \qquad C = \epsilon_o N_o^2 \quad \text{(Farad/m)}$$

$$Z_c = (L/C)^{1/2} \ (\Omega), \qquad Z_o = (\mu_o/\epsilon_o)^{1/2} \ (\Omega)$$

$$L_a = \mu_o\alpha_m \frac{1}{N_o^2} \left(\frac{\partial\phi}{\partial n}\right)^2 \quad \text{(Henry/m)}$$

$$C_a = \epsilon_o\alpha_e \left(\frac{\partial\phi}{\partial n}\right)^2 \quad \text{(Farad/m)}$$

$$N_o^2 = \frac{2\pi}{\ell n(D_c/N_c)} \quad \text{(Dimensionless)}$$

$$N_c = R_c(x_o,y_o) \ R_c(-x_o,-y_o) \ R_c[x'(x_o,-y_o), \ y'(x_o,-y_o)]$$
$$R_c[x'(-x_o,y_o), \ y'(-x_o,y_o)]$$

$$D_c = R_c(-x_o,y_o)\ R_c(x_o,-y_o)\ R_c[x'(x_o,y_o),\ y'(x_o,y_o)]$$

$$R_c[x'(-x_o,-y_o),\ y'(-x_o,-y_o)]$$

$$R_c(x,y) = [(x_c - x)^2 + (y_c - y)^2] \qquad (m)$$

$$x'(x,y) = x \cos 2\alpha + (\ell - y) \sin 2\alpha$$

$$y'(x,y) = -y \cos 2\alpha + 2\ell \cos^2\alpha - x \sin 2\alpha$$

$$-\frac{\partial\phi}{\partial n} = \frac{1}{2}\left[\left(-\frac{\partial\phi_o}{\partial n}\right)_{max} + \left(-\frac{\partial\phi_o}{\partial n}\right)_{av}\right] \quad (m^{-1}) \quad \text{(Section III)}$$

$$\left(-\frac{\partial\phi_o}{\partial n}\right)_{av} = \frac{N_o^2}{2\pi a}\sum_{i=1}^{4} \epsilon_i\left[\tan^{-1}\frac{2a - x_i\cos\alpha - (\ell - y_i)\sin\alpha}{|x_i \sin\alpha - (\ell - y_i)\cos\alpha|}\right.$$

$$\left. + \tan^{-1}\frac{x_i\cos\alpha + (\ell - y_i)\sin\alpha}{|x_i \sin\alpha - (\ell - y_i)\cos\alpha|}\right] \quad \text{(Section III)}$$

$$(x_1,y_1) = (x_o,y_o),\ (x_2,y_2) = (-x_o,-y_o),\ (x_3,y_3) = (-x_o,y_o),$$

$$(x_4,y_4) = (x_o,-y_o)$$

$$\epsilon_1 = \epsilon_2 = 1,\ \epsilon_3 = \epsilon_4 = -1$$

$$\left(-\frac{\partial\phi_o}{\partial n}\right)_{max} = \text{maximum}\left\{\frac{N_o^2}{\pi}\left[\frac{\cos\theta(x_o,y_o)}{R(x_o,y_o)} + \frac{\cos\theta(-x_o,-y_o)}{R(-x_o,-y_o)}\right.\right.$$

$$\left.\left. - \frac{\cos\theta(-x_o,y_o)}{R(-x_o,y_o)} - \frac{\cos\theta(x_o,-y_o)}{R(x_o,-y_o)}\right]\right\} \quad \text{(Section III)}$$

$[(-\partial\phi_o/\partial n)_{max}$ = maximum of $-\partial\phi_o/\partial n$ over the aperture.]

$$\cos\theta(x,y) = \frac{(\ell - y)\cos\alpha - x\sin\alpha}{R(x,y)}$$

$$R(x,y) = \left((x_A - x)^2 + (\ell - y - x_A\tan\alpha)^2\right)^{1/2} \quad (m)$$

where $J_z(z)$ (Amps/m) $\left[= (H_{ext})_\phi\right]$, $\sigma(z)$ (Coulombs/m^2) $\left[= \epsilon_o(E_{ext})_n\right]$ are the short-circuited current density (= magnetic field) and charge density (= ϵ_o × electric field) respectively averaged over the aperture at z; and are obtained by solving the external interaction problem with all the apertures short-circuited. $\alpha_m = \alpha_{m\phi\phi}(m^3)$, $\alpha_e(m^3)$ are the magnetic and electric polarizabilities respectively calculated in Appendix B; x_o, y_o (m) are the coordinates of the center of the pneumatic duct (fig. 10); $x_c = x_o - a_D$, $y = y_o$ and a_D (m) is the radius of the pneumatic duct; α and ℓ(m) are defined in figure 10; a(m) and d(m) are defined in figure 15 and x_A(m) is the x-coordinate of a point in the aperture. $(-\partial\phi_o/\partial n)_{av}$ was obtained by integrating $(-\partial\phi_o/\partial n)_{av}$ over the aperture and dividing by 2a, i.e., $(-\partial\phi/\partial n)_{av} = (1/2a)\int_A(-\partial\phi/\partial n)\, dc_A$.

The current induced on the unshielded cables is given by

$$I_c(z,y) = \frac{I(z)}{N_o^2}\frac{\partial\phi_o}{\partial x}d_c \quad \text{(Amps)} \qquad (85)$$

$$\frac{\partial\phi_o}{\partial x} = -\frac{N_o^2 x_o}{\pi}\left[\frac{1}{R^2(x_o,y_o)} - \frac{1}{R^2(x_o,-y_o)}\right] \quad (m^{-1})$$

$$R^2(x_o,\pm y_o) = x_o^2 + (y \mp y_o)^2 \quad (m^2)$$

where I(z) (Amps) is the current induced on the pneumatic duct at z, d_c (m) is the diameter of an unshielded cable and

y (m) is the coordinate at the center of an unshielded cable (the x-coordinate is taken equal to zero).

As an example we consider the E-4 aircraft specific dimensions of which are given in figure 16. In addition we choose the following average dimensions (fig. 10)

$$x_o = 0.4 \text{ m} \qquad 2a = 0.9 \text{ m}$$

$$y_o = 0.2 \text{ m} \qquad \alpha = 35°$$

$$\ell = 0.8 \text{ m}$$

In order to obtain a simplified formula and upper bound for the current induced on the pneumatic duct, we assume that the equivalent transmission line in figure 15 is matched on both sides, i.e., $Z_L = Z_R = Z_{ce} = (L'/C')^{1/2}$. In this case the current is given by Equations 62

$$I \leq \frac{L_w}{2}\left\{\frac{\tilde{V}'_{eq}}{Z_{ec}} + \tilde{I}'_{eq}\right\}$$

$$= \frac{kL_w}{4d}\left|\frac{\partial\phi}{\partial n}\right|\left\{\alpha_m\left(\frac{Z_c}{Z_{ec}}\right)\tilde{J}_z + \alpha_e\, c\tilde{\sigma}\right\} \qquad (86)$$

where

$$\tilde{J}_z = \frac{1}{L_w}\int_{L_1}^{L_2} |J_z(z)|\,dz$$

$$\tilde{\sigma} = \frac{1}{L_w}\int_{L_1}^{L_2} |\sigma(z)|\,dz$$

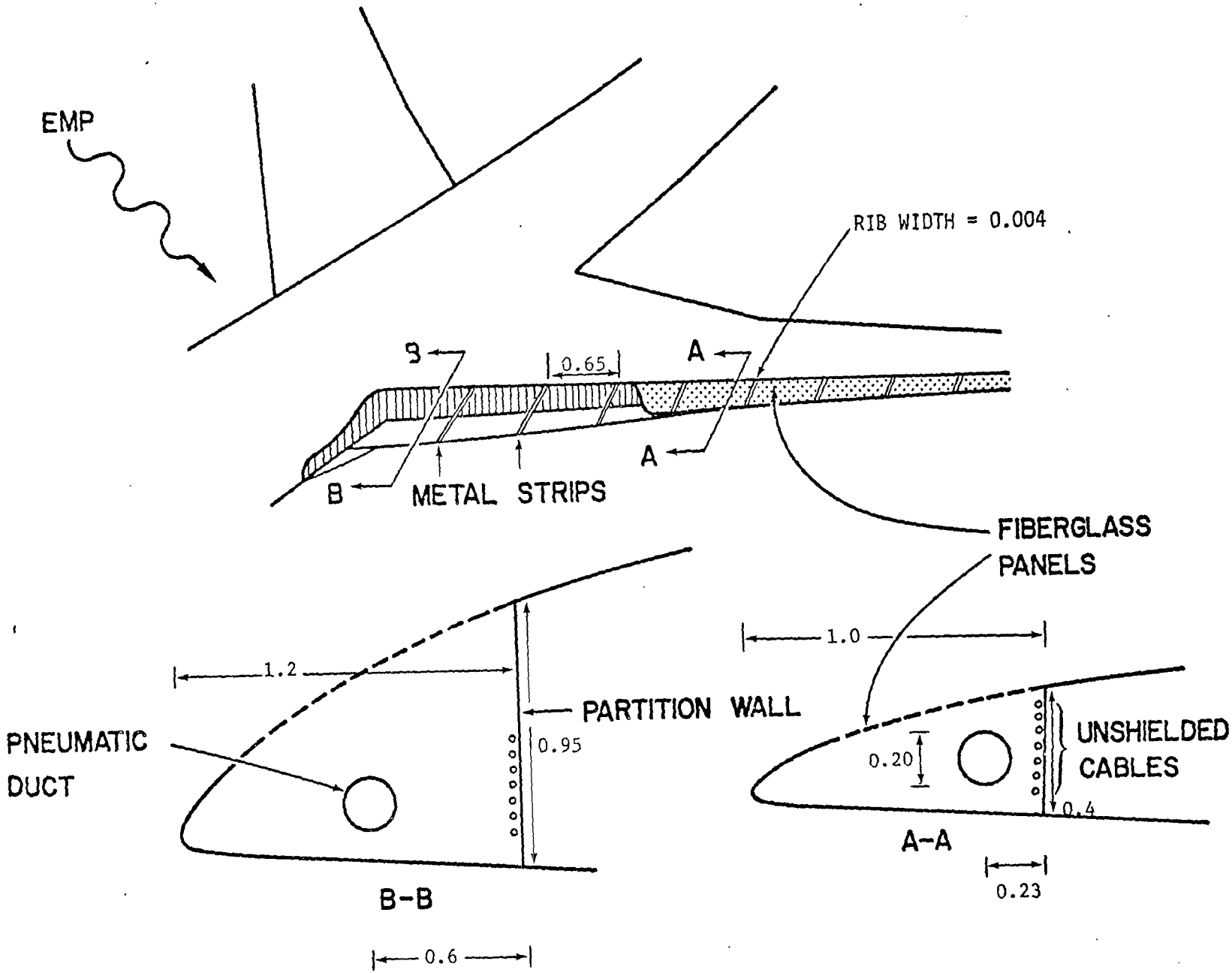

Figure 16. Geometry for the EMP Penetration Problem Corresponding to an E-4 Aircraft. (All Dimensions in Meters)

and $J_z(z)$, $\sigma(z)$ are, as we indicated earlier, the short-circuited current and charge densities respectively averaged over the aperture, L_w the length over which the array of apertures extends and c = speed of light = 3×10^8 m/sec. For the specific dimensions corresponding to the E-4 aircraft we can find

$$\left|\frac{\partial \phi}{\partial n}\right| = 3.5\ m^{-1}, \quad Z_c = 0.15\ Z_o$$

$$L' = 0.20\ \mu_o, \quad C' = 4.63\ \epsilon_o$$

$$Z_{ec} = (L'/C')^{1/2} = 0.21\ Z_o$$

$Z_c/Z_{ec} = 0.71$, $\alpha_m = \alpha_e \approx \pi a^2 d/2$ (from Appendix B)

$$V'_{eq} = -0.0835\ ikJ_z(z), \quad I'_{eq} = 0.557\ ik\sigma(z)$$

$$\tilde{V}'_{eq} = 0.0835\ k\tilde{J}_z, \qquad \tilde{I}'_{eq} = 0.557\ k\tilde{\sigma}$$

and Equation 86 gives

$$I \leq 0.28(kL_w)(0.71\ \tilde{J}_z + c\tilde{\sigma}) \quad \text{(Amps)} \tag{87}$$

$$V = 0.21\ Z_o I \qquad (Z_o = 377\Omega) \quad \text{(Volts)}$$

J_z is measured in Amps/m, σ in Coulombs/m^2, $k = (2\pi f/c)$ in m^{-1} and L_w in m.

In order to calculate the current induced on the cables we choose a representive one with y = 0.4 m, i.e., in the middle of the partition wall. Then the current induced on this cable is given by Equation 87 where I(z) is given by Equation 86 and

$$\frac{1}{N_o^2}\left|\frac{\partial \phi_o}{\partial x}\right| = 0.392 \ .$$

Thus

$$I \leq 0.11\ (kL_w)d_c\ (0.71\ \tilde{J}_z + c\tilde{\sigma})$$

where d_c is the diameter of the cable.

In order to obtain J_z and σ we should solve the external interaction problem with all apertures short-circuited, for frequencies such that $2kb << 1$ (b is shown in figure 15). Notice that the zeroth order magnetic and electric fields we considered in Section II in the calculation of the dipole moments are static fields only in the sense that they are the zeroth order terms in an expansion of the true magnetic and electric fields in kb. These zeroth order terms depend on the external interaction problem which can be solved for a range of frequencies satisfying the condition $2kb << 1$. However, one should examine if this condition is also sufficient to cause a rapid decay of the higher order modes generated at the aperture sites. For a coaxial cable with radii a_1, a_2, condition $k_o(a_1 - a_2) < 1$ insures that the higher order modes become negligible over a distance $a_1 - a_2$. In our case the average linear dimension of the triangular cavity is the same order of magnitude as 2b and consequently condition $2kb << 1$ is sufficient to cause a very rapid decay of the higher modes.

APPENDIX A

DIPOLE MOMENTS FOR AN APERTURE IN A PLANAR SCREEN

In this appendix we consider an interesting aspect of the problem of electromagnetic penetration through an aperture in a perfectly conducting screen. We show that in the low frequency limit ($kd << 1$ where d is the linear dimension of the aperture) the transmitted far zone electromagnetic field can be obtained by considering the far zone electromagnetic field due to an electric dipole $\underline{p}$ and a magnetic dipole $\underline{m}$, placed in front of the conducting screen with the aperture short-circuited such that

$$\underline{m} = \frac{-1}{i\omega\mu_o} \int_A (\hat{n} \times \underline{E})\, dS$$

$$\underline{p} = -\frac{\varepsilon_o}{2} \int_A \underline{r}_s \times (\hat{n} \times \underline{E})\, dS \qquad \text{(A-1)}$$

where $\underline{r}_s$ is the two-dimensional radius vector in the aperture and $\underline{E}$ is the true aperture electric field for the original penetration problem. Equations A-1 of course are not new but we include our proof here for completeness.

We begin with the well-known equation (fig. A1)

$$\underline{E}(\underline{r}_s) = -2\int_A (\hat{n} \times \underline{E}) \times \nabla_s g\, dS \qquad \text{(A-2)}$$

where $g = \frac{e^{ikR}}{4\pi R}$ $\qquad R = |\underline{r} - \underline{r}_o|$.

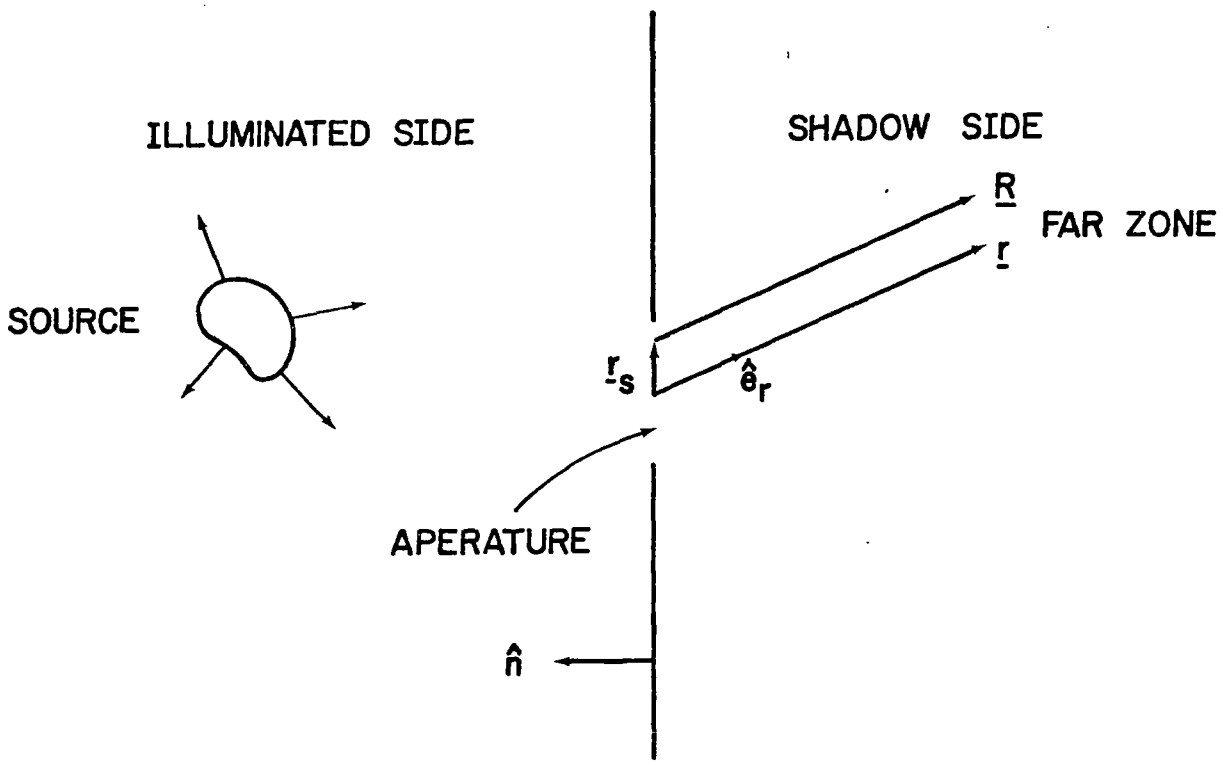

Figure A1. Geometry for the Calculation of $\underline{m}$ and $\underline{p}$ in Terms of the Aperture Electric Field

In the far zone we have

$$\nabla_s g \approx \frac{ike^{ikR}}{4\pi R} \frac{\underline{r}_s - \underline{r}}{R} \approx \frac{ike^{ikr-ik\hat{e}_r\cdot\underline{r}_s}}{4\pi r} (-\hat{e}_r)$$

and for $|k\hat{e}_r \cdot \underline{r}_s| << 1$ (low frequency limit)

$$\nabla_s g \approx - \frac{ike^{ikr}}{4\ r} (1 - ik\hat{e}_r \cdot \underline{r}_s)\ \hat{e}_r \qquad \text{(A-3)}$$

Using Equation A-3 in A-2 we obtain

$$\underline{E}(\underline{r}) = \frac{ike^{ikr}}{2\pi r} \int_A (\hat{n} \times \underline{E})\ dS \times \hat{e}_r + \frac{k^2 e^{ikr}}{2\pi r} \int_A (\hat{n} \times \underline{E})(\hat{e}_r \cdot \underline{r}_s)\ dS \times \hat{e}_r \qquad \text{(A-4)}$$

A magnetic dipole in free space produces a far zone electric field (ref. 5)

$$\underline{E}^{(m)} = Z_o k^2 \frac{e^{ikr}}{4\pi r} (\underline{m} \times \hat{e}_r; \qquad \text{(A-5)}$$

Comparing Equation A-5 with the first term in Equation A-4 we understand that

$$\underline{m} = 2 \frac{i}{Z_o k} \int_A (\hat{n} \times \underline{E})\ dS$$

$$= \frac{2i}{\omega\mu_o} \int_A (\hat{n} \times \underline{E})\ dS \qquad \text{(free space)}$$

---

5. Papas, C. H., Theory of Electromagnetic Wave Propagation, McGraw-Hill Book Company, New York, 1965.

and in front of an infinite perfectly conducting screen

$$\underline{m} = \frac{-1}{i\omega\mu} \int_A (\hat{n} \times \underline{E})\, dS$$

which is identical to the first of Equations A-1. To show the truth of the second equation requires some manipulation. First we recall that

$$\nabla_s \cdot (\underline{\underline{A}}\, \underline{r}_s) = (\nabla_s \cdot \underline{\underline{A}})\, \underline{r}_s + \underline{\underline{A}}^T \qquad \text{(A-6)}$$

where $\underline{\underline{A}}^T$ is the transposed of $\underline{\underline{A}}$.

Employing Equation A-6 we can write

$$\int_A \underline{r}_s \underline{K}\, dS = \int_A \nabla_s \cdot (\underline{K}\, \underline{r}_s \underline{r}_s) dS - \int_A \nabla_s \cdot (\underline{K}\, \underline{r}_s) \underline{r}_s dS. \qquad \text{(A-7)}$$

If $\underline{K} = \hat{n} \times \underline{E}$ then $\underline{E} \cdot \hat{u} = 0$, where $\hat{u}$ is a tangential vector along the rim of the aperture. If we use this property and the two-dimensional form of Gauss' law we can set the first integral on the right-hand side of Equation A-7 equal to zero. If we now use

$$\nabla_s \cdot (\underline{K}\, \underline{r}_s) = (\nabla_s \cdot \underline{K})\, \underline{r}_s + \underline{K}$$

and the continuity Equation 20 in Section II we can rewrite Equation A-7 as

$$\int_A \underline{r}_s\, \underline{K} dS = -\int_A \underline{K}\, \underline{r}_s dS + i\omega\mu_o \int \hat{n} \cdot \underline{H}\, \underline{r}_s \underline{r}_s\, dS\ . \qquad \text{(A-8)}$$

Next we observe that

$$(\underline{r}_s \times \underline{K}) \times \hat{e}_r = \underline{K}\, \underline{r}_s \cdot \hat{e}_r - \underline{r}_s\, \underline{K} \cdot \hat{e}_r$$

and combine this with Equation A-8 to obtain

$$\int_A \underline{K}\, \underline{r}_s dS \cdot \hat{e}_r = \frac{1}{2} \int_A (\underline{r}_s \times \underline{K})\, dS \times \hat{e}_r$$

$$+ \frac{i\omega\mu_o}{2} \int \hat{n} \cdot \underline{H}\, \underline{r}_s \underline{r}_s\, dS \cdot \hat{e}_r \,. \qquad \text{(A-9)}$$

With the aid of Equation A-9 we can now rewrite the second term in Equation A-4 as

$$E^{(2)} = \left\{ \frac{k^2 e^{ikr}}{4\pi r} \int_A [\underline{r}_s \times (\hat{n} \times \underline{E})] dS \times \hat{e}_r \right\} \times \hat{e}_r \qquad \text{(A-10)}$$

where we have discarded the integral involving $\underline{H}$ as higher order. Recalling that the far zone electric field due to an electric dipole $\underline{p}$ in free space is (ref. 5)

$$\underline{E}^{(p)} = \frac{k^2 e^{ikr}}{4\pi r} (\hat{e}_r \times \underline{p}) \times \hat{e}_r$$

we can use Equation A-10 to deduce that

$$\underline{p} = -\frac{\epsilon_o}{2} \int_A \underline{r}_s \times (\hat{n} \times \underline{E})\, dS$$

if $\underline{p}$ is placed in front of an infinite perfectly conducting screen. Notice that $\underline{r}_s \times (\hat{n} \times \underline{E}) = \hat{n}(\underline{r}_s \cdot \underline{E})$ and the expression for $\underline{p}$ coincides with Equation 27.

APPENDIX B

CALCULATION OF DIPOLE MOMENT POLARIZABILITIES FOR A PERIODIC CONFIGURATION OF RECTANGULAR APERTURES

In this appendix we give an approximate calculation for the magnetic and electric dipole polarizabilities for a periodic configuration of rectangular apertures in a perfectly conducting screen (fig. B1). (In reference 6 a categorization of the types of apertures is given, including one-dimensional arrays or gratings.) As we explained at the end of section II, for the calculation of the equivalent voltage and current sources we need only know $\alpha_{m\phi\phi}$ and α_e since $\alpha_{m\phi z}$ is zero and α_{mzz} does not enter into the calculation for the equivalent sources. However, in this appendix, in addition to the magnetic polarizability $\alpha_{mxx}(= \alpha_{m\phi\phi})$ and electric polarizability α_e we also calculate α_{mzz} for future reference.

1. MAGNETIC POLARIZABILITIES

By definition

$$\underline{m} = -\underline{\underline{\alpha}}_m \cdot \underline{H}_{ext}, \quad \underline{m} = -\int_A \underline{r}_s \, \hat{n} \cdot \underline{H} dS \tag{B-1}$$

where $\underline{H}_{ext}$ is the short-circuited magnetic field, $\underline{r}_s$ is the radius vector in the plane of the aperture and $\hat{n} \cdot \underline{H}$ is the normal component of the aperture magnetic field. ($\hat{n}$ points into the source region.) We are interested in calculating α_{mxx} and α_{mzz}, i.e.,

$$m_x = -\underline{\underline{\alpha}}_m \cdot \underline{H}_{ext} = -\alpha_{mxx}(H_{ext})_x = -\int x \, \hat{n} \cdot \underline{H} dS \tag{B-2}$$

---

6. Baum, C. E., K. C. Chen and B. K. Singaraju, Categorization of the Types of Apertures, Interaction Note 219, Air Force Weapons Laboratory, January 1975.

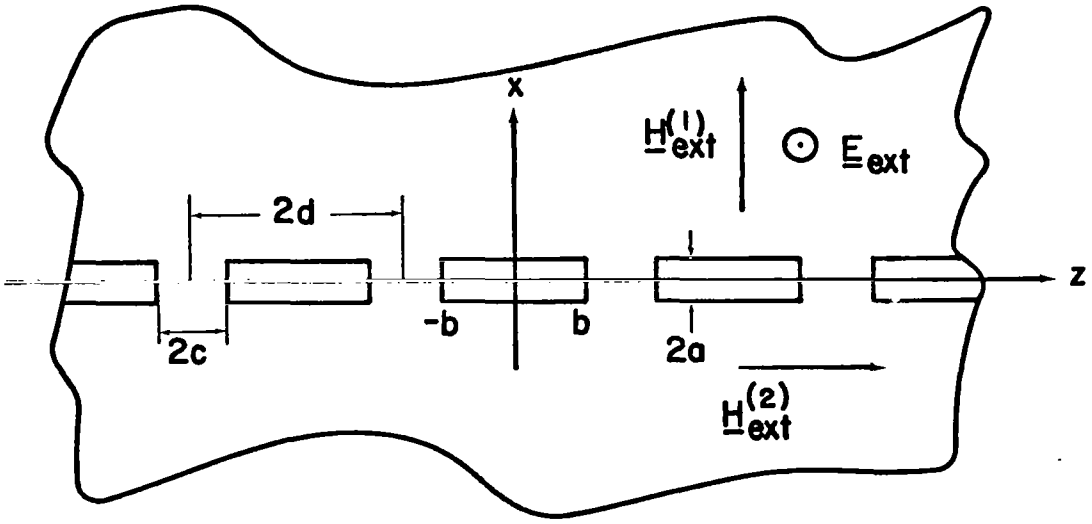

Figure B1. A Periodic Array of Rectangular Apertures

$$m_z = -\alpha_{mzx}(H_{ext})_x - \alpha_{mzz}(H_{ext})_z$$

$$= -\alpha_{mzz}(H_{ext})_z = -\int z\ \hat{n} \cdot \underline{H} dS \qquad \text{(B-3)}$$

since $\alpha_{mzx} = \alpha_{mxz} = 0$. Thus we must first calculate $\hat{n} \cdot \underline{H}$ for $\underline{H}_{ext}$ in the x- and z-directions.

a. $\alpha_m \equiv \alpha_{mxx} = \alpha_{m\phi\phi}$

For the geometry depicted in figure B-1 with $\underline{H}_{ext} = H_{ext}\ \hat{e}_x$ we can introduce a scalar potential such that $\underline{H} = \nabla\Psi$. Because of symmetry the total magnetic field at $z = \pm d, \pm 3d$ etc. lies entirely in the xy plane and consequently $\partial\Psi/\partial z = 0$ at $z = \pm d$, $\pm 3d$ etc. At $y = 0$ and outside the apertures $\partial\Psi/\partial y = 0$ since the total magnetic field is tangential to the conducting screen. By introducing appropriate Green's functions such that $\partial G/\partial z = 0$ at $z = \pm d, \pm 3d$ etc. and $\partial G/\partial y = 0$ at $y = 0$ we can employ Green's theorem for the region $y > 0$ $-d \leq z \leq d$ and $y > 0$ $-d \leq z \leq d$ to derive the following integral relationships

$$y > 0 \quad \Psi(x,y,z) = \Psi^{ext}(x,y,z) + \int_{-a}^{a} dx' \int_{-b}^{b} G_1(x',0,z';\ x,y,z)$$

$$\cdot \frac{\partial}{\partial y'} \Psi(x',y',z')\Big|_{y'=0} dz'$$

$$y < 0 \quad \Psi(x,y,z) = -\int_{-a}^{a} dx' \int_{-b}^{b} G_2(x',0,z';\ x,y,z)$$

$$\cdot \frac{\partial}{\partial y'} \Psi(x',y',z')\Big|_{y'=0} dz' \qquad \text{(B-4)}$$

where

$$\psi^{ext} = H_{ext}\, x$$

$$\nabla'^2 G_1(\underline{r}';r) = \delta(\underline{r}' - r) \qquad y', y \geq 0$$

$$\frac{\partial G}{\partial y'} = 0 \quad y' = 0 \qquad \frac{\partial G_1}{\partial z'} = 0 \quad z' = \pm d$$

$$\nabla'^2 G_2(\underline{r}';\underline{r}) = \delta(\underline{r}' - \underline{r}) \qquad y', y \leq 0$$

$$\frac{\partial G}{\partial y'} = 0 \quad y' = 0 \qquad \frac{\partial G_2}{\partial z'} = 0 \quad z' = \pm d$$

G_1 and G_2 have the following explicit forms

$$G_1(x',y',z';\, x,y,z) = -\sum_{n=0}^{\infty} \int_{-\infty}^{\infty} dp\, \frac{\epsilon_n}{2\pi d}\, \frac{1}{s}\, e^{-ys} \cosh y's$$

$$e^{ip(x'-x)} \cos k_n z' \cos k_n z, \quad 0 < y' < y$$

$$G_2(x',y',z';\, x,y,z) = G_1(x',-y',z';\, x,-y,z) \qquad 0 > y' > y \tag{B-5}$$

where $\epsilon_n = 1$, $n \neq 0$, $\epsilon_o = 0.5$, $s = (k_n^2 + p^2)^{1/2}$, $k_n = n\pi/d$. The above formulas can be obtained by expanding $\delta(z' - z)$ in a cosine series, i.e.,

$$\delta(z' - z) = \sum_{n=0}^{\infty} (\epsilon_n/d) \cos k_n z' \cos k_n z,$$

writing $\delta(x' - x)$ as

$$(1/2\pi) \int_{-\infty}^{\infty} dp\ e^{ip(x'-x)},$$

setting

$$G = \sum_{n=0}^{\infty} \int_{-\infty}^{\infty} dp\ g_n(y',y,p)\ e^{ip(x'-x)}\ \cos k_n z'\ \cos k_n z$$

and solving for $g_n(y',y,p)$ in the usual manner.

In order to obtain an integral equation for $\partial\Psi/\partial y'\big|_{y' = 0} = H_y(x',0,x')$ we let $y \to 0$ in Equation B-4 and use the boundary conditions: Ψ, H_y continuous in the aperture. Thus we can derive the following integral equation

$$\int_{-a}^{a} dx' \int_{-b}^{b} (G_1 + G_2)\ H_y\ dz' = -H_{ext}\ x$$

or

$$\int_{-a}^{a} dx' \int_{-b}^{b} K(x',x;\ z',z)\ H_y\ dz' = H_{ext}\ x \qquad \text{(B-6)}$$

where

$$K(x',x;\ z',z) = \sum_{n=0}^{\infty} \frac{\epsilon_n}{\pi d} \int_{-\infty}^{\infty} \frac{dp}{\left(p^2 + k_n^2\right)^{1/2}} e^{ip(x'-x)}\ \cos k_n z'\ \cos k_n z \qquad \text{(B-7)}$$

For $k_n \neq 0$ we can use the well-known relationship

$$2K_o(k_n|x' - x|) = \int_{-\infty}^{\infty} \frac{e^{ip(x'-x)}}{\left(p^2 + k_n^2\right)^{1/2}} dp$$

where $K_o(u)$ is the modified Bessel function of the second kind of zeroth order to rewrite Equation B-7 as

$$K(x',x;\ z',z) = K^{(o)}(x',x;\ z',z) + \frac{2}{\pi d} \sum_{n=1}^{\infty} K_o(k_n|x' - x|)$$

$$\cos k_n z' \cos k_n z \qquad \text{(B-8)}$$

In order to solve Equation B-6 approximately, we guess a functional for H_y that satisfies the edge condition and symmetry properties. (A similar approach can be found in reference 7). The simplest form is

$$H_y(x',z') = -\frac{\alpha}{\pi} \frac{x' H_{ext} d}{(a^2 - x'^2)^{1/2}(b^2 - z'^2)} \qquad \text{(B-9)}$$

In order to determine α, which is assumed to be independent of position, we integrate both sides of Equation B-6 from 0 to a and -b to b. The resulting expression involves several integrals. First we consider n = 0

---

7. Lam, J., Metal Skin Panel Joints, AIP Memos, Memo 3, Air Force Weapons Laboratory, November 1976.

We have

$$\int_{-b}^{b} \frac{dz'}{(b^2 - z'^2)^{1/2}} = \pi , \quad \int_{-b}^{b} dz = 2b$$

and

$$\int_{o}^{a} \frac{x' \, e^{ipx'}}{(a^2 - x'^2)^{1/2}} = 2i \int_{o}^{a} \frac{x' \sin px'}{(a^2 - x'^2)^{1/2}} \, dx' = i\pi a \, J_1(|p|a) \, \frac{p}{|p|}$$

according to reference 8,

$$\int_{o}^{a} e^{-ipx} \, dx = \frac{1}{ip} \, (1 - e^{-ipa}) .$$

Next the integral

$$I = \int_{-\infty}^{\infty} \frac{J_1(|p|a) \, (1 - e^{-ipa})}{p^2} \, dp$$

arises. (Notice that $(p^2 + k_n^2)^{1/2} = |p|$ for $n = 0$.) We can write

---

8. Gradshteyn, I. S. and I. M. Ryzhik, Table of Integrals, Series and Products, Academic Press, New York, 1965, p. 419, 3.753-5.

$$I = 2\int_0^\infty \frac{J_1(pa)(1 - \cos pa)}{p^2}\, dp$$

To evaluate this integral we define

$$I_1(\alpha,\beta) = \int_0^\infty \frac{J_1(p\alpha)(1 - \cos p\beta)}{p^2}\, dp$$

and

$$\frac{\partial I_1(\alpha,\beta)}{\partial \beta} = \int_0^\infty \frac{J_1(p\alpha)\ \sin p\beta}{p}\, dp = \frac{\beta}{\alpha} \qquad \beta \leq \alpha$$

according to reference 7. Thus

$$I_1(\alpha,\beta) = \frac{\beta^2}{2\alpha} + c(\alpha) = \frac{\beta^2}{2\alpha}$$

since $I(\alpha,0) = 0$ and $I = I_1(a,a) = 1/2$. Next we consider the integrals corresponding to $n \neq 0$. We have

$$\int_{-b}^{b} \frac{\cos k_n z'}{(b^2 - z'^2)^{1/2}}\, dz' = 2\int_0^1 \frac{\cos k_n u}{(1 - u^2)^{1/2}} = \pi J_o(k_n b)$$

according to reference 8.

Since $K_o(k_n|x' - x|)$ involves both x' and x the following two-dimensional integral arises

$$I_2 = \int_0^a dx \int_{-a}^a \frac{x' K_o(k_n|x' - x|)}{(a^2 - x'^2)^{1/2}} dx'$$

To reduce I_2 to a one-dimensional integral, we set $x' - x = u$, $x' = x'$ and refer to figure B2 to transform I_2 to

$$I_2 = \int_0^a du K_o(k_n u) \int_u^a \frac{x'\,dx'}{(a^2 - x'^2)^{1/2}} + \int_{-a}^0 du K_o(k_n|u|)$$

$$\int_u^{u+a} \frac{x'\,dx'}{(a^2 - x'^2)^{1/2}} + \int_{-2a}^{-a} du K_o(k_n|u|) \int_{-a}^{u+a} \frac{x'\,dx'}{(a^2 - x'^2)^{1/2}}$$

$$= 2a^2 \int_0^1 K_o(k_n a u)(1 - u^2)^{1/2}\,du - 4a^2 \int_0^1 K_o(2k_n a u)$$

$$\cdot (u - u^2)^{1/2}\,du \equiv 2a^2 S(k_n a), \qquad k_n = \frac{n\pi}{d} \tag{B-10}$$

Using the above results we obtain

$$\alpha = \frac{\pi b/d}{\frac{\pi b}{d} + \sum_{n=1}^{\infty} \frac{8}{n\pi} J_o\left(\frac{n\pi b}{d}\right) \sin\left(\frac{n\pi b}{d}\right) S_n\left(\frac{n\pi a}{d}\right)} \tag{B-11}$$

where S_n is given by Equation B-10.

With the aid of Equations B-2 and B-9 we find

$$\alpha_m \equiv \alpha_{mxx} = \frac{1}{H_{ext}} \int_{-a}^a dx \int_{-b}^b dz\; x \frac{\alpha}{\pi} \frac{xd\,H_{ext}}{(a^2 - x^2)^{1/2}(b^2 - z^2)^{1/2}}$$

$$= (\pi a^2 d/2)\alpha \tag{B-12}$$

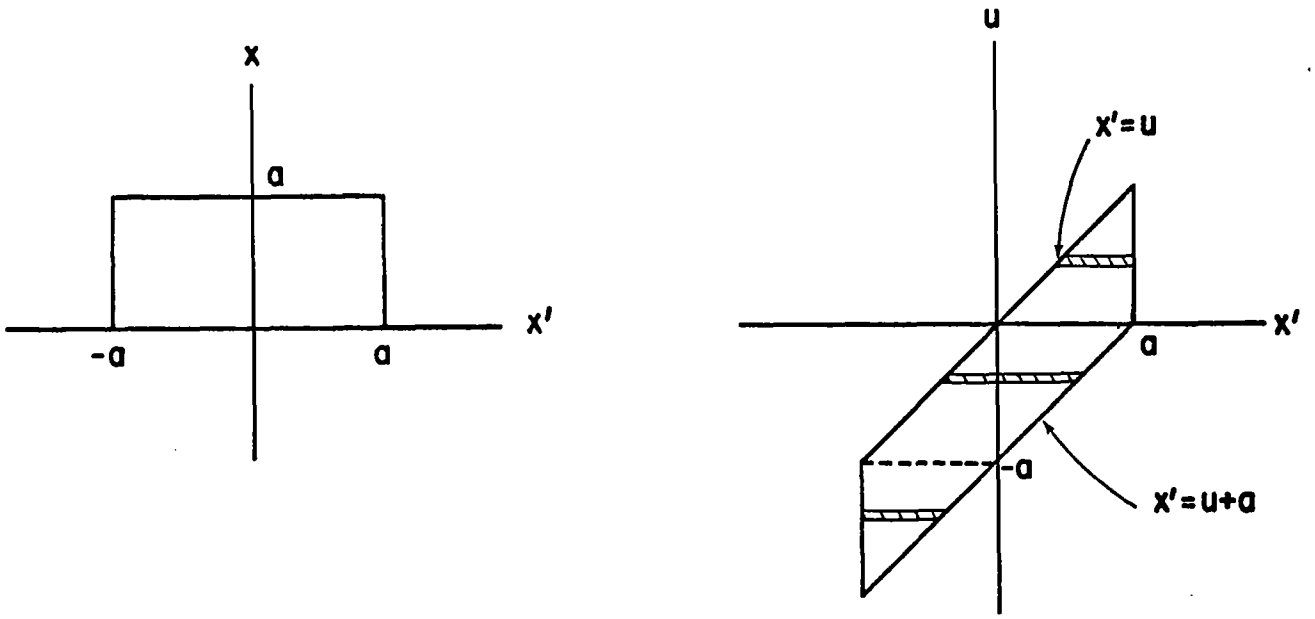

Figure B2. Coordinate Transformation for the Evaluation of a Two-Dimensional Integral in Appendix B

and

$$\alpha_m' \equiv \alpha_{mxx}/2d = \frac{\pi a^2 \alpha}{4} \qquad \text{(B-13)}$$

For an infinite slot the magnetic polarizability per unit length α_m^∞ is $\pi a^2/4$ and

$$\frac{\alpha_m'}{\alpha_m^\infty} = \alpha \qquad \text{(B-14)}$$

where α is given by Equation B-11.

When b = d Equation B-11 gives $\alpha = 1$, i.e., $\alpha_m' = (\alpha_{mxx}/2d) = \alpha_m^\infty$ as expected. For the E-4 aircraft considered in section IV (fig. 16) $b/d = 0.65/0.654 \approx 0.994$, $a/d \approx 1$, i.e., $\alpha_m' \approx \alpha_m^\infty = \pi a^2/4$. We can show this by bounding the sum in Equation B-11. A simple calculation gives Sum < 0.14 << 1 and consequently $\alpha \approx 1$. This can also be seen from the graphs in figure B3 where $\alpha_e'/\alpha_m^\infty$ is plotted versus b/d with a/b as parameter. When $b/d = 0.1$ the apertures are far enough from each other to be viewed as isolated. In this case α_{mxx} ($= 2d\alpha_m' = \pi a^2 d\alpha/2$) should represent the magnetic polarizability for a rectangular aperture in an infinite conducting screen in the presence of the short-circuited $\underline{H}_{ext} = H_{ext}\,\hat{e}_x$. This polarizability has been calculated in reference 4 and its value is used in the table that follows.

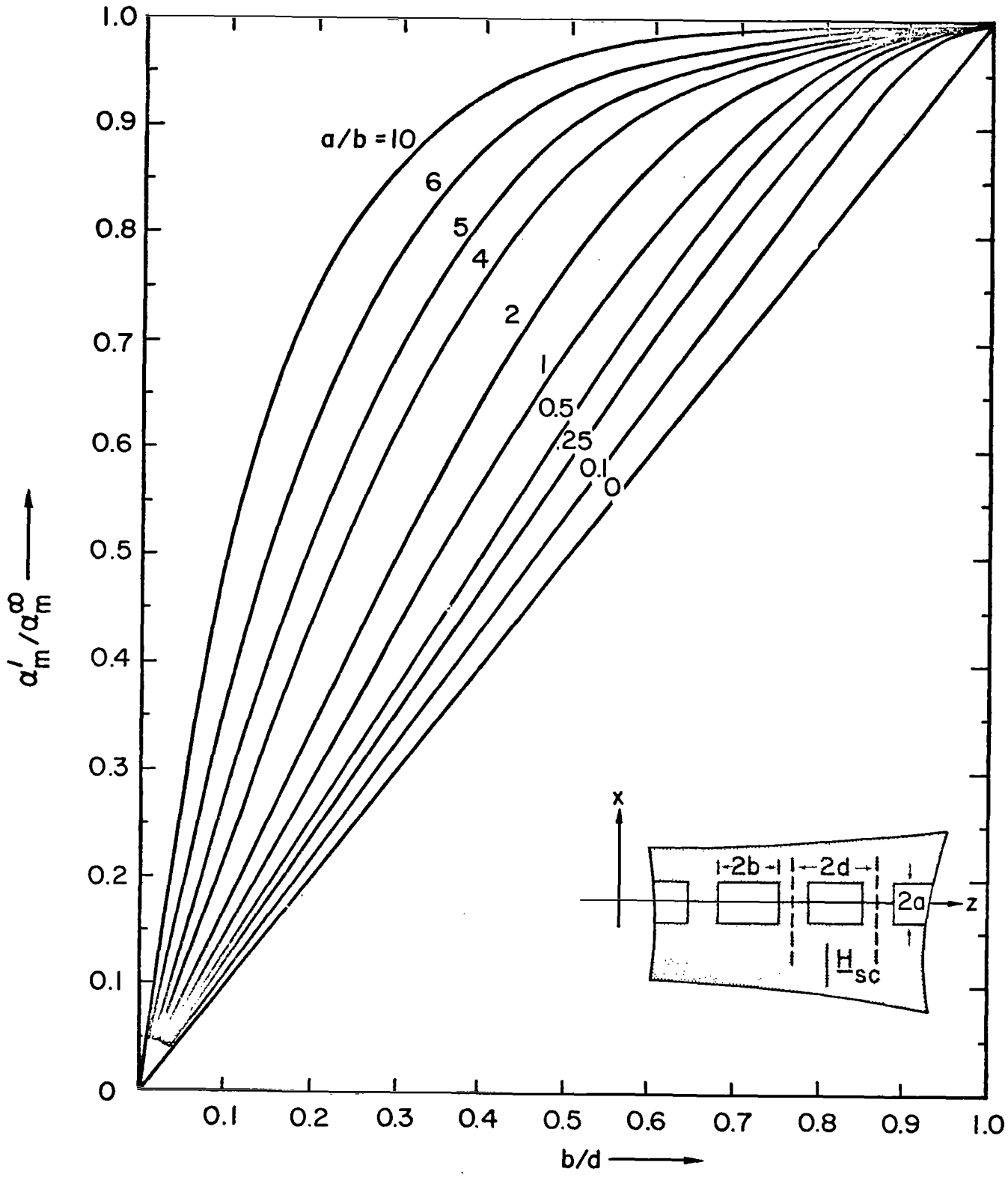

Figure B3. $\alpha_m' \equiv \alpha_{mxx}/2d$, $\alpha_{mxx} \equiv$ the xx Component of Aperture Magnetic Polarizability for an Infinite Periodic Array of Rectangular Apertures with $\underline{H}_{sc} = H_{sc}\hat{e}_x$
$\alpha_m^\infty \equiv$ Magnetic Polarizability per Unit Length for an Infinite Slot

α_{mxx}/a^3			
a/d	a/b	Ref. 4	This Report (b/d = 0.1)
0.005	0.05	33.7	35.3
0.01	0.1	16.2	17.9
0.025	0.25	6.91	7.45
0.05	0.5	3.67	3.96
0.08	0.8	2.48	2.61
0.1	1	2.08	2.22
0.125	1.25	1.75	1.85
0.2	2	1.26	1.34
0.4	4	0.818	0.886
1.0	10	0.518	0.560
2.0	20	0.393	0.393

The agreement between the results in reference 4 and this report is good and it improves as a/b increases. When $a/b < 1$ the magnetic field $H_{ext}\,\hat{e}_x$ is perpendicular to the long side of the rectangle whereas $a/b > 1$ corresponds to a magnetic field parallel to the long side. In the next subsection we calculate the magnetic polarizability α_{mzz} for a magnetic field in the z-direction and we find that again the agreement improves for large a/b, i.e., when the magnetic field is perpendicular to the long side. For the case displayed in the above table, i.e., for b/d = 0.1 our results overestimate the true polarizability results and it is expected that this is also true for larger b/d.

b. α_{mzz}

For the calculation of α_{mzz} we consider a short-circuited external magnetic field in the z-direction. Again we introduce a scalar potential Ψ such that $\underline{H} = \nabla\Psi$. In order to derive an integral equation for $\partial\Psi/\partial y = H_y$ we choose $\Psi = 0$ and $G = 0$ at $z = \pm d, \pm 3d$ etc. We also recall that $\partial\Psi/\partial y = 0$ on the metallic part of the screen and impose the condition $\partial G/\partial y = 0$ at $y = 0$. Under these circumstances Green's theorem leads to the following integral relationships.

$$y > 0 \quad \Psi(x,y,z) = \Psi^{ext}(x,y,z) + \int_{-a}^{a} dx' \int_{-b}^{b} G_1(x',0,z';\ x,y,z) \cdot \frac{\partial}{\partial y'} \Psi(x',y',x') \Big|_{y'=0} dz'$$

$$y < 0 \quad \Psi(x,y,z) = -\int_{-a}^{a} dx' \int_{-b}^{b} G_2(x',0,z';\ x,y,x) \cdot \frac{\partial}{\partial y'} \Psi(x',y',z') \Big|_{y'=0} dz' \qquad \text{(B-15)}$$

where

$$\Psi^{ext} = H_{ext}\, z$$

$$G_1(x',y',z';\ x,y,z) = -\sum_{n=1}^{\infty} \int_{-\infty}^{\infty} \frac{dp}{2\pi ds} \frac{1}{s} e^{-ys} \cosh y's \; e^{ip(x'-x)} \sin k_n z' \sin k_n z \qquad 0 < y < y'$$

$$G_2(x',y',z';\ x,y,z) = G_1(x',-y',z';\ x,-y,z) \qquad 0 > y' > y \tag{B-16}$$

where $s = \left(p^2 + k_n^2\right)^{1/2}$, $k_n = n\pi/d$.

By allowing the observation point to approach the screen and invoking the continuity of Ψ and $\partial\Psi/\partial y$ in the aperture we can derive the following integral equation

$$\int_{-a}^{a} dx' \int_{-b}^{b} K(x',z';\ x,z)\ H_y dz' = H_{ext}\ z \tag{B-17}$$

where

$$K(x',z';\ x,z) = \sum_{n=1}^{\infty} \frac{2}{\pi d} K_o(k_n|x' - x|)\ \sin k_n z'\ \sin k_n z$$

$K_o(u)$ is the modified Bessel function of the second kind and of zeroth order and $k_n = n\pi/d$.

In order to find an approximate solution for Equation B-17 we assume a simple form for H_y that satisfies symmetry requirements and edge conditions, i.e.,

$$H_y(x,z) = -\beta \frac{z\ H_{ext}\ b}{(a^2 - x^2)^{1/2}\ (b^2 - z^2)^{1/2}} \tag{B-18}$$

and integrate both sides of Equation B-17 from -a to a and 0 to b. The resulting equation involves the following integrals

$$\int_0^b \int_{-b}^b \frac{z' \sin k_n z' \sin k_n z}{(b^2 - z'^2)^{1/2}} dz'dz = \frac{\pi b}{k_n} (1 - \cos k_n b) J_1(k_n b)$$

according to reference 8 (p. 419, 3.753-5) and

$$I = \int_{-a}^{a} dx \int_{-a}^{a} \frac{K_o(k_n|x' - x|)}{(a^2 - x'^2)^{1/2}} dx'.$$

If we introduce the transformation $x' - x = u$, $x' = x'$ and refer to figure B4 we find

$$I = \int_o^{2a} K_o(k_n u) \left[\frac{\pi}{2} - \sin^{-1}\left(\frac{u - a}{a}\right)\right] du$$

$$+ \int_{-2a}^{o} K_o(k_n|u|) \left[\sin^{-1}\left(\frac{u + a}{a}\right) + \frac{\pi}{2}\right] du$$

$$= 2a \int_o^2 K_o(k_n a u) \left[\frac{\pi}{2} + \sin^{-1}(1 - u)\right] du \equiv 2aS(k_n a) \quad \text{(B-19)}$$

and

$$\beta = \frac{1}{\sum_{n=1}^{\infty} \frac{4}{\pi n} (1 - \cos k_n b) J_1(k_n b) S(k_n a)} \quad \text{(B-20)}$$

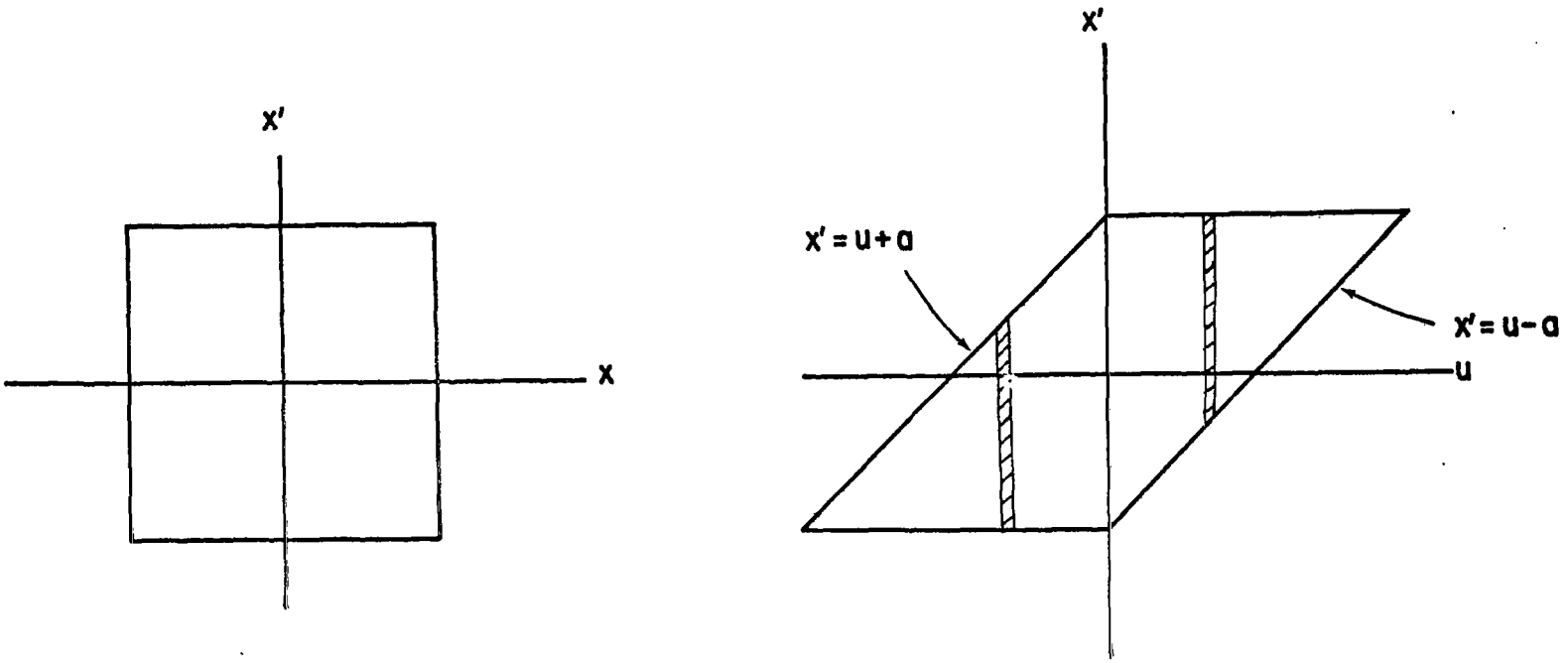

Figure B4. Coordinate Transformation for the Evaluation of a Two-Dimensional Integral
Appendix B

where $S_n(k_n a)$ is defined by Equation B-19. With the aid of Equations B-18 and B-3 we find

$$\alpha_{mzz} = \frac{1}{H_{ext}} \int_{-a}^{a} dx \int_{-b}^{b} dz \; \frac{z^2 b \, H_{ext}}{(a^2 - x^2)^{1/2} (b^2 - z^2)^{1/2}}$$

as

$$\alpha_{mzz} = \beta \frac{\pi^2 b^3}{2} \qquad \text{(B-21)}$$

where β is given by Equation B-20.

In figure B5 we have plotted $\alpha_{mzz}/(\pi^2 b^3/2)$ versus b/d with a/b as parameter. When b/d = 0.1 the apertures are far enough from each other to be considered isolated and α_{mzz} should correspond to the polarizability of a rectangular aperture in a perfectly conducting screen in the presence of a short-circuited magnetic field $\underline{H}_{ext} = H_{ext} \hat{e}_z$. We can then compare the results of our calculations to those obtained in reference 4 where the polarizability for a rectangular aperture in a perfectly conducting screen was calculated. In the table that follows we display our results for b/d = 0.1 and those obtained in reference 4 (which of course correspond to b/d → 0). Notice that the normalized quantity displayed is α_{mzz}/b^3 rather than α_{mzz}/a^3 because we also want to compare our results for $\underline{H}_{ext} = H_{ext} \hat{e}_z$ to those obtained in the first subsection of this appendix, i.e., when $\underline{H}_{ext} = H_{ext} \hat{e}_x$ where the roles of a and b are interchanged.

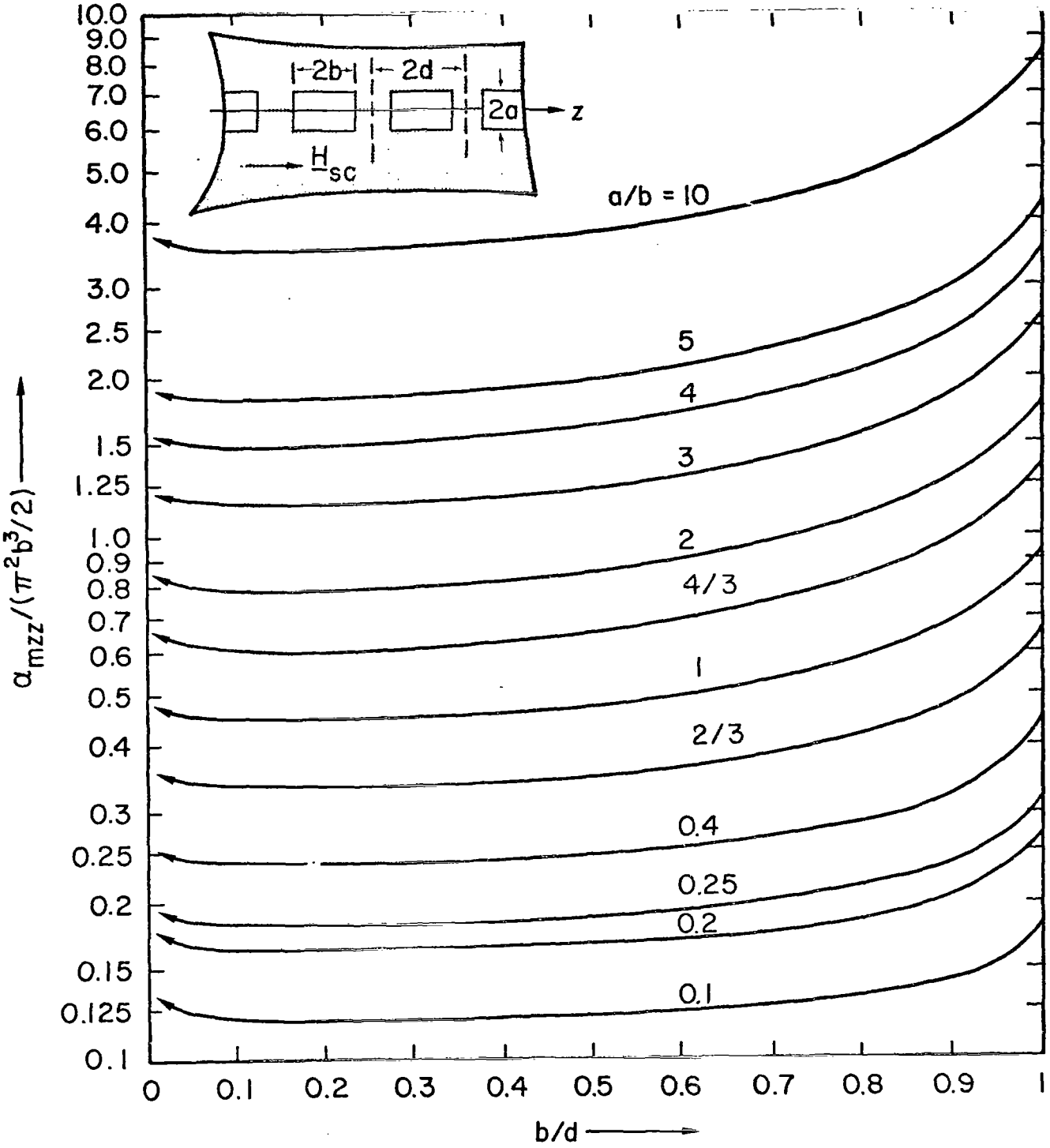

Figure B4. α_{mzz} ≡ The zz Component of Aperture Magnetic Polarizability for an Infinite Periodic Array of Rectangular Apertures with $\underline{H}_{sc} = H_{sc}\hat{e}_z$

α_{mzz}/b^3			
a/d	b/a	Ref. 4	This Report (b/d = 0.1)
2	0.05	33.7	33.8
1	0.1	16.2	16.4
0.4	0.25	6.91	7.32
0.2	0.5	3.67	3.91
0.125	0.8	2.48	2.65
0.1	1	2.08	2.22
0.8	1.25	1.75	1.88
0.5	2	1.26	1.35
0.025	4	0.818	0.894
0.01	10	0.518	0.589
0.005	20	0.393	0.464

The above table shows good agreement between the results in reference 4 and this report. We observe that the agreement is excellent for large a/b, i.e., when the magnetic field is perpendicular to the long side whereas the opposite is true for $\underline{H}_{ext}$ in the x-direction as we found in the previous subsection of this appendix. In the present case, i.e., for $\underline{H}_{ext}$ in the z-direction a large a/b, say 20, corresponds to a long aperture and α_{mzz} should approximately be equal to $(\pi/2)\ b^2a$. Indeed $\alpha_{mzz} = 33.8\ b^3 = 33.8\ b^2(a/20) = 1.69\ b^2a \lesssim (\pi/2)\ b^2a$. The above table shows that the calculation of α_{mzz} in this appendix overestimates its value for b/d = 0.1 and it is expected that this is also true for larger b/d.

2. ELECTRIC POLARIZABILITY

In order to calculate the electric polarizability we recall Equations 28 and $\underline{p} = \epsilon_o \alpha_e \underline{E}_{ext}$. $\underline{E}_{ext}$ is the short-circuited external electric field (fig. B1). Thus

$$\alpha_e = - \frac{1}{E_{ext}} \int_{-a}^{a} dx \int_{-b}^{b} \Psi(x,0,z)\, dz \qquad \text{(B-22)}$$

where Ψ is a scalar potential such that $\underline{E} = -\nabla\Psi$ and $\Psi = 0$ on the metallic part of the screen. Due to symmetry the total electric field $\underline{E}$ at $z = \pm d, \pm 3d$ etc. lies entirely in the xy plane and consequently $\partial\Psi/\partial z = 0$ at $z = \pm d, \pm 3d$. Thus in order to derive an integral equation for $\Psi(x,0,z)$ we introduce appropriate Green's functions such that $G = 0$ at $y = 0$ and $\partial G/\partial z = 0$ at $z = \pm d, \pm 3d$ etc. Application of Green's theorem results in the following integral relationships

$$y > 0 \qquad \Psi(\underline{r}) = \Psi^{ext}(\underline{r}) - \int_A \Psi(\underline{r}') \left.\frac{\partial G_1}{\partial y'}\right|_{y'=0} dS'$$

$$\Psi(\underline{r}) = \int_A \Psi(\underline{r}') \left.\frac{\partial G_2}{\partial y'}\right|_{y'=0} dS' \qquad \text{(B-23)}$$

where A is the $-d \leq z \leq d$, $-a \leq x \leq a$ aperture,

$$G_1(x',y',z';\ x,y,z) = -\sum_{n=0}^{\infty}\int_{-\infty}^{\infty} dp\ \frac{\epsilon_n}{2\pi ds}\ e^{-ys}\ \sin h(y's)$$

$$e^{ip(x'-x)}\ \cos k_n z'\ \cos k_n z \qquad 0 < y' < y$$

$$G_2(x',y',z';\ x,y,z) = -G_1(x',-y',z;\ x,-y,z) \qquad 0 > y' > y$$

(B-24)

and $\epsilon_o = 1/2$, $\epsilon_n = 1$ for $n \neq 0$, $s = \left(p^2 + k_n^2\right)^{1/2}$, $k_n = n\pi/d$. If we allow the observation point $\underline{r}$ to approach the screen ($y = 0$) we obtain

$$\left.\frac{\partial G_1}{\partial y'}\right|_{y'=0,y=0} = -\delta(x' - x)\ \delta(z' - z)$$

$$\left.\frac{\partial G_2}{\partial y'}\right|_{y'=0,y=0} = \delta(x' - x)\ \delta(z' - z)$$

and Equations B-23 give two identities since $\Psi^{ext} = 0$ at $y = 0$. Thus as $y \to 0$ Equations B-23 cannot be used to calculate $\Psi(x,0,z)$ as we did with the magnetic polarizabilities. However, we can still use Equations B-23 to derive the following set of integral relationships.

$$\frac{\partial \Psi(\underline{r})}{\partial y} = \frac{\partial \Psi_{inc}(\underline{r})}{\partial y} - \frac{\partial}{\partial y}\int_A \Psi(\underline{r}')\ \left.\frac{\partial G_1}{\partial y'}\right|_{y'=0} dS' \qquad y > 0$$

$$\frac{\partial \Psi(\underline{r})}{\partial y} = \frac{\partial}{\partial y}\int_A \Psi(\underline{r}')\ \left.\frac{\partial G_2}{\partial y'}\right|_{y'=0} dS' \qquad y < 0$$

(B-25)

As $y \to 0$ we use Equations B-25 and the continuity of Ψ and $\partial\Psi/\partial y$ at the aperture to derive the following equation:

$$\left.\frac{\partial \Psi_{inc}}{\partial y}\right|_{y=0} = \left[\frac{\partial}{\partial y}\int_A \Psi(x',0,z')\left[\frac{\partial G_1}{\partial y'} + \frac{\partial G_2}{\partial y'}\right]_{y'=0} dS'\right]_{y=0}$$

$$= \left[\frac{\partial}{\partial y}\int_A dS'\ \Psi(x',0,z') \sum_{n=0}^{\infty} \frac{\epsilon_n}{\pi d} \int_{-\infty}^{\infty} dp\ \sinh ys\ e^{ip(x'-x)}\right.$$

$$\left.\cos k_n z' \cos k_n z\right]_{y=0}$$

or

$$-E_{ext} = \int_A dS'\ \Psi(x',0,z') \sum_{n=0}^{\infty} \frac{\epsilon_n}{\pi d} \int_{-\infty}^{\infty} dp\ \sqrt{p^2 + k_n^2}\ e^{ip(x'-x)}$$

$$\cos k_n z' \cos k_n z \qquad \text{(B-26)}$$

Again we guess the simplest form of $\Psi(x,0,z)$ that satisfies the symmetry requirements and edge conditions

$$\Psi(x,0,z) = -\frac{2\gamma d}{\pi b^2} E_{ext} (a^2 - x'^2)^{1/2} (b^2 - z'^2)^{1/2} \qquad \text{(B-27)}$$

and use this expression in Equation B-26. To determine γ we integrate both sides of Equation B-26 from -a to a and -b to b and do the resulting integrations:

$$\int_{-a}^{a} (b^2 - x'^2)^{1/2} \, e^{ip(x'-x)} \, dx' = e^{-ipx} \, \frac{\pi a}{p} \, J_1(pa)$$

$$\int_{-b}^{b} (b^2 - z'^2)^{1/2} \cos k_n z' \, dz' = \frac{\pi b}{k_n} \, J_1(k_n b) \quad (= \pi b^2/2 \text{ for } n = 0)$$

$$\int_{-a}^{a} e^{-ipx} \, dx = \frac{2 \sin pa}{p} \, , \quad \int_{-b}^{b} \cos k_n z \, dz = \frac{2}{k_n} \sin k_n b$$

$$(= 2b \text{ for } n = 0)$$

If we define

$$f(k_n a) \equiv \int_0^{\infty} \frac{du}{u^2} \sin u \, J_1(u) \, (u^2 + k_n^2 \, a^2)^{1/2} \qquad \text{(B-28)}$$

and notice that $f(o) = 1$ (ref. 8, p. 743, 6.693) we obtain

$$\gamma = \frac{1}{1 + \sum_{n=1}^{\infty} \left(\frac{2}{\pi n}\right)^2 \left(\frac{d}{b}\right)^2 J_1(k_n b) \, \sin(k_n b) \, f(k_n a)} \qquad \text{(B-29)}$$

Thus the electric polarizability α_e is determined with the aid of Equations B-22 and B-27

$$\alpha_e = \frac{1}{E_{ext}} \int_{-a}^{a} dx \int_{-b}^{b} \frac{2\gamma d\, E_{ext}}{\pi b^2} (a^2 - x^2)^{1/2} (b^2 - z^2)^{1/2} dz$$

$$= \frac{2\gamma d}{\pi b^2} E_{ext} \left(\frac{\pi ab}{2}\right)^2 \frac{1}{E_{ext}} = \frac{\pi a^2 d}{2} \gamma$$

$$\alpha_e' \equiv \alpha_e / 2d = \gamma. \qquad \text{(B-30)}$$

For an infinite slot, α_e^∞ (polarizability per unit length) is equal to $\pi a^2/4$ and

$$\frac{\alpha_e'}{\alpha_e^\infty} = \gamma. \qquad \text{(B-31)}$$

When b = d Equation B-29 gives $\gamma = 1$ and from Equation B-31 we obtain $\alpha_e' = \alpha_e^\infty = \pi a^2/4$ as expected. For the E-4 aircraft (fig. 16) $b/d = 0.65/0.654 \approx 0.994$, $a/d \approx 1$ and one can show that $\beta \lesssim 1$ and $\alpha_e' \lesssim \alpha_e^\infty = \pi a^2/4$. To exhibit the dependence of electric polarizability on b/d and b/a we have plotted in figure B6 $\alpha_e'/\alpha_e^\infty$ versus b/d with b/a as parameter. When b/d = 0.1 the apertures are far enough from each other to be considered isolated and $\alpha_e = 2d\alpha_e'$ corresponds to the electric polarizability for a rectangular aperture in a perfectly conducting screen in the presence of a short-circuited $\underline{E}_{ext} = E_{ext}\, \hat{e}_y$. Reference 4 has calculated this polarizability and the following table allows a comparison between our results and those in reference 4.

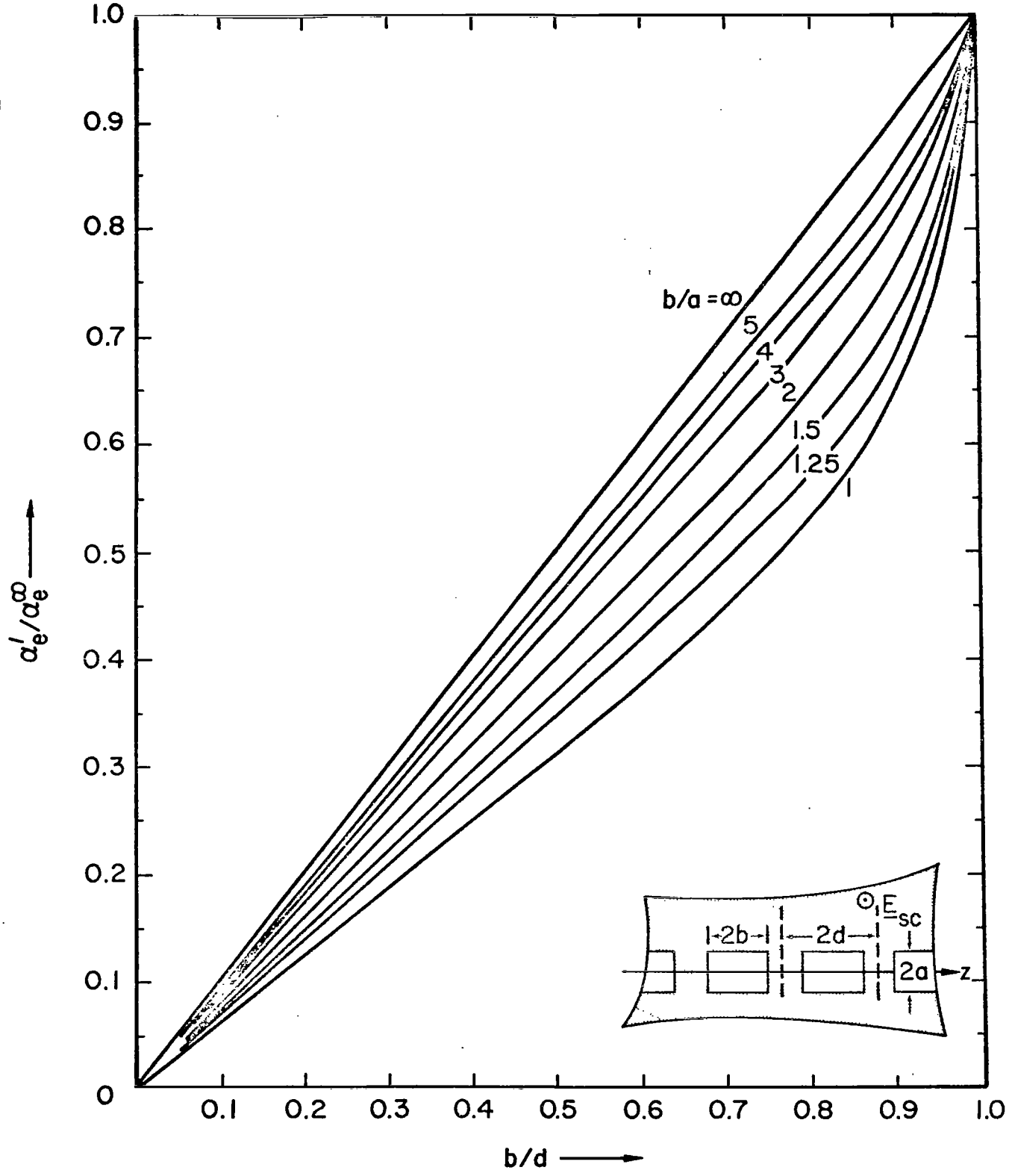

Figure B6. α_e' ≡ (Aperture Electric Polarizability)/2d for an Infinite Periodic Array of Rectangular Apertures, α_e^∞ ≡ Electric Polarizability per Unit Length for an Infinite Slot

α_e/b^3			
a/d	a/b	Ref. 4	This Report (b/d = 0.1)
0.1	1	0.910	0.955
0.15	1.5	1.62	1.74
0.2	2	2.38	2.52
0.25	2.5	3.14	3.39
0.3	3	3.92	4.10
0.4	4	5.48	5.81
0.5	5	6.95	7.41
1	10	14.9	15.5
2	20	30.6	31.2

The agreement is very good and it is excellent for large a/b. The calculations for α_e in this report overestimates its value for b/d = 0.1 and it is expected that this is also true for larger b/d.

REFERENCES

1. Sancer, M. I., S. Siegel and A. D. Varvatsis, "Foundation of the Magnetic Field Integral Equation Code for the Calculation of Electromagnetic Pulse External Interaction with Aircraft," Interaction Note 320, Air Force Weapons Laboratory, January 1973.

2. Van Bladel, J. Electromagnetic Fields, McGraw-Hill Book Company, New York, p. 418, 1964.

3. Lee, K.S.H. and C. E. Baum, "Application of Modal Analysis to Braided-Shield Cables," Interaction Note 132, Air Force Weapons Laboratory, January 1973.

4. Latham, R. W., Small Holes in Cable Shields, Air Force Weapons Laboratory, Interaction Note 118, September 1972.

5. Papas, C. H., Theory of Electromagnetic Wave Propagation, McGraw-Hill Book Company, New York, 1965.

6. Baum, E.C., K. C. Chen and B. K. Singaraju, Categorization of the Types of Apertures, Interaction Note 219, Air Force Weapons Laboratory, January 1975.

7. Lam, J., Metal Skin Panel Joints, AIP Memos, Memo 3, Air Force Weapons Laboratory, November 1976.

8. Gradshteyn, I.S. and I. M. Ryzhik, Table of Internal Series and Products, Academic Press, New York, 1965.